KARFI

Final Proposal

Undergraduate Design Team

University of Maryland - College Park

40th Annual Vertical Flight Society Student Design Competition

Sponsored by: Sikorsky, a Lockheed Martin Company

Alfred Gessow Rotorcraft Center
Department of Aerospace Engineering
University of Maryland
College Park, MD 20742

Remi Hensel
Undergraduate Student (Team Lead)
henselr@umd.edu

Justin Hathaway
Undergraduate Student
jhathawa@umd.edu

Dogyu Jun
Under*graduate Student*
djun1127@umd.edu

Jeremy Page
Undergraduate Student
jpage193@umd.edu

Reilly Keenen
Undergraduate Student
rkeenen@umd.edu

Ao Huang
Undergraduate Student
ahuang18@umd.edu

Brett Sweeney
Undergraduate Student
bsweens@umd.edu

Dr. Vengalatore Nagaraj
Faculty Advisor
vnagaraj@umd.edu

Dr. James D. Baeder
Faculty Advisor
baeder@umd.edu

Spencer Fishman
Instructor
fish@umd.edu

Students will receive credits for ENAE482 (Aeronautical Systems Design) for their contributions

ACKNOWLEDGEMENTS

The design team wishes to acknowledge the following people for their invaluable discussion, guidance, and support throughout the course of this project.

University of Maryland Faculty

Dr. Vengalattore T. Nagaraj — Research Scientist, Department of Aerospace Engineering, University of Maryland, College Park

Dr. James D. Baeder — Professor, Department of Aerospace Engineering, University of Maryland, College Park

Dr. Inderjit Chopra — Director of Alfred Gessow Rotorcraft Center, University of Maryland, College Park

Spencer Fishman — Instructor, Department of Aerospace Engineering, University of Maryland, College Park

Alfred Gessow Rotocraft Research Center Graduate Students

Matt Arace

Vivek Uppoor

Nathan T. O'Brien

Paolo Arias

Xavier Delgado

Bumseok Lee

Alfred Gessow Rotorcraft Center
Department of Aerospace Engineering
University of Maryland
College Park, MD 20742 U.S.A.

To the Vertical Flight Society:

The members of the University of Maryland Undergraduate Student Design Team hereby grant VFS full permission to distribute the enclosed Executive Summary and Final Proposal for the 40th Annual Design Competition as they see fit.

Thank you,

The UMD Undergraduate Design Team

Contents

List of Figures

List of Tables

1 Introduction

The 2023 Vertical Flight Society (VFS) Request for Proposal (RFP) calls for a unique aircraft with two principal design challenges. First, the RFP asks for a transport aircraft capable of high-speed flight. The RFP also requests that this aircraft be capable of vertical take-off and landing (VTOL). All figures in the following report are given in English units since it is the industry standard in the United States.

In response to this year's RFP, the University of Maryland's undergraduate team has developed *Karfi*. *Karfi* is a thrust-compounding two-speed transmission tiltrotor capable of carrying a crew of three and a payload over a large mission radius in high speed cruise. The name *Karfi* comes from the Norse word for a mid-size cargo and troop ship. Much like how the Vikings possessed unprecedented naval superiority, the *Karfi* demonstrates a never before seen combination of airborne capabilities. Some of *Karfi*'s notable aspects are as follows. Fuselage-embedded turboshaft engines increase the wing bending frequency and thus the whirl flutter onset speed The aircraft'sΠ-tail integrates embedded turbofan engines leading to a lower frontal area and better thrust efficiency due to boundary layer ingestion. It also houses a two-speed transmission allowing the aircraft to keep its proprotor tip speed under the drag divergence Mach number.

1.1 RFP Requirements

The RFP emphasizes several key themes: a conjunction of high speed cruise and VTOL capabilities, management of downwash and outwash effects and threat avoidance measures for operation in highly contested zones. The RFP also encourages the use of innovative solutions while balancing the respective technology readiness levels (TRL). The main attributes and requirements for the aircraft and report are detailed in Tables 1.1 and 1.2.

1.1.1 High Speed and VTOL Capabilities

The RFP asks for a transport aircraft that can carry 6,000 lb (2,722 kg) of payload and mission equipment package (MEP) and cruise at 450 kts (833.4 km/h) at an altitude of at least 20,000 ft (6,096 m). The aircraft must operate in these conditions for a mission radius of 500 nm (926 km) where 50 nm (92.6 km) is performed as a low altitude high speed penetration. The RFP also requests that the aircraft possess VTOL capabilities, a complex challenge at this scale and speed. Implementing high speed and VTOL capabilities pose diametrically opposed requirements when it comes to vehicle design.

Large open rotor systems are not commonly used for high speed flight. This stems from the fact that for high speed forward flight, drag, specifically the L/D ratio, is a determining factor of the achievable cruise speed. If the rotor tip speed exceeds the drag divergence Mach number, drag increases exponentially. As a result, high speed rotor systems tend to require small rotors. On the other hand, a vehicle capable of VTOL operations usually requires large open rotor systems in order to minimize disk loading, downwash effects on ground personnel, and rotorwash-induced foreign object debris. As a result, the vehicle design proposed must have a balance that allows VTOL operations in unprepared surfaces without sacrificing high speed efficiency.

1.1.2 Threat Avoidance

The RFP explicitly asks for air vehicle concepts which incorporate technologies and design features enabling threat avoidance to meet military needs in highly-contested environments. To this end, careful consideration of what a highly-contested environment entails and potential solutions for improving threat avoidance is necessary, whether it be minimizing radar cross section or implementing countermeasures.

External Dimensions

Footprint: 94.05 ft x 66.87 ft
(28.67 m x 20.38 m)

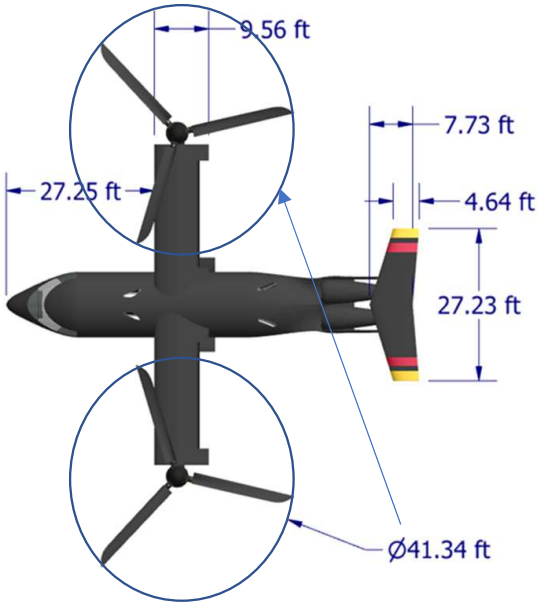

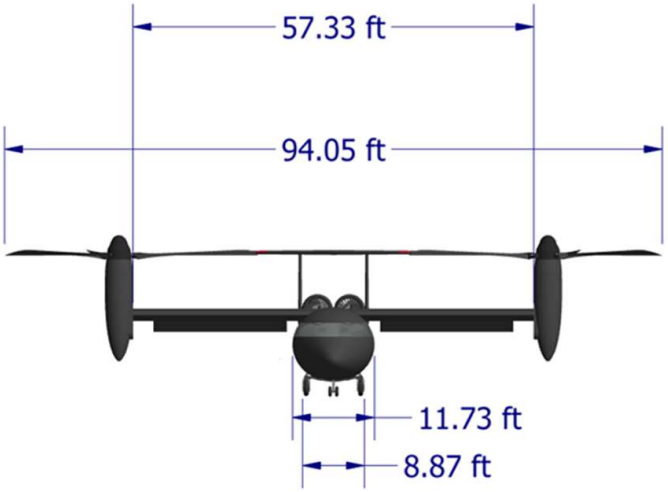

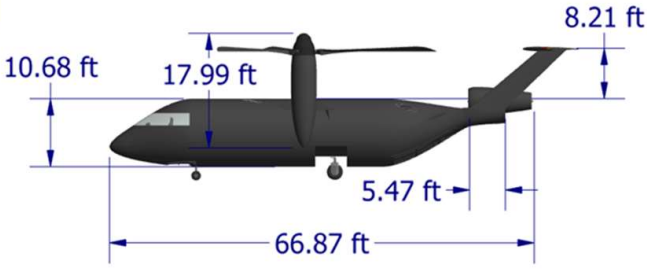

GTOW	**46,829 lb** (21,241 kg)
Empty Weight	**29,374 lb** (13,324 kg)
Payload	**5,000 lb** (2,268 kg)
Fuel Weight	**10,235 lb** (4643 kg)

UNIVERSITY OF MARYLAND

KARFI

RFP Requirements	Proposed Solutions	Section
VTOL aircraft capable of a minimum cruise speed of 450 kts at minimum altitude of 20,000 ft (6,095 m)	Vehicle uses a combination of turbofans and a two-speed rotor system to provide the necessary thrust without enduring considerable drag penalties	3, 6, 7
Mitigate severity of downwash/outwash effects on ground personnel and landing environment	The vehicle was designed to operate during VTOL operations for a disk loading of 19.5 lb/ft^2 (933.66 Pa). Additionally, the turbofans were placed so as to be away from areas of operational use	3, 5, 9
Military level threat avoidance technologies and design features for use in highly contested environments	The vehicle's mission equipment package was designed to incorporate threat avoidance technologies. Additionally, the structural design of the aircraft incorporates technologies to mitigate radar cross section	5, 8, 9
The vehicle must contain a cargo bay with dimensions of 6.5 ft (1.98 m) height, 8 ft (2.43 m) width and 30 ft (9.14 m) length	The vehicle is sized to incorporate a 6.5 ft (1.98 m) high, 8 ft (2.43 m) wide and 30 ft (9.14 m) long cargo bay	3, 5, 8
The vehicle must be capable of carrying a payload of 5,000 lbs (2,268 kg), a crew of 3 totaling 750 lbs (340 kg) and a mission equipment package of 1,000 lbs (455 kg)	The vehicle was sized with theses parameters held constant so as to ensure that all design choices reflect this need	3, 9
Minimize vulnerability of the propulsion system to foreign object debris ingestion during VTOL operations	The aircraft's engines are mounted high in the fuselage rather than in the nacelle and disk loading was reduced	3, 5, 8
The aircraft shall have a mission radius of action of 500 nm (926 km) following the specified mission profile	The vehicle sizing code was built around the mission profile provided by the RFP to ensure its ability to complete the required mission.	3, 6
All technologies used in aircraft must achieve TRL 6 by 2027 and TRL 9 by 2035	All technologies used in the vehicle have at the very least been fully "bench-tested" at a 1:1 scale	2, 4, 5, 6, 7, 8, 9

Table 1.1: RFP Compliance

RFP Deliverables	Chapter
Conceptual Design Trade Studies	2.2, 3.3 and 3.4
Vehicle Description	1
Power Available at Engine Output Shaft per Power Setting	7.1.1
Energy Consumption at Engine Output Shaft per Power Setting	7.1.1
Total Aircraft Power Required vs Gross Weight	6.2
Download as a Percentage of Gross Weight	6.2
Total Air Vehicle Figure of Merit vs Gross Weight	6.1
Total Power Required vs Airspeed from Hover to Maximum Continuous Power Speed	6.2 and 6.3
Mission Performance Data	6
General Arrangement	1.1.1
Inboard Profile	
Structural Arrangement	8.1
Subsystem Functional Schematics	8.2
Vertical Flight Aerodynamic Data	6.1
Forward Flight Edgewise Mode Aerodynamic Data	6.1
Airframe Equivalent Areas	6.1
Limit load factor structural and aerodynamic envelope at structural design gross weight and maximum gross weight	6.4
Component Design Loads	6.4
Mass Properties Data	11
Manufacturing and Cost Data	2.2 and 10

Table 1.2: RFP Deliverables

1.1.3 Mission Profile

The specific mission profile the RFP presents is composed of 12 different flight segments that are completed over a total distance of 1,000 nm (1,852 km). This mission, illustrated in Figure 1, is that of a resupply operation into a hostile environment. Consequently, the aircraft is required to carry a total payload of 5,000 lbs (2,267.96 kg) and three crew members weighing a total of 750 lbs (340.2 kg) over the entirety of the mission which is detailed below.

1. 10-minute flight idle.
2. 2-min Hover In Ground Effect (HIGE) takeoff (close to surface, less than 1 rotor diameter)
3. Cruise-climb at best climb speed (VBROC) where range credit may be taken for the total Radius of Action (ROA) in flight legs 4 and 6

4. Cruise 450 nm (833 km) at no less than 20,000 ft (6,096 m) ISA conditions or best cruise altitude at the best range speed (V_{BR}) or no less than 450 KTAS (833 km/hr)
5. Descend to 2,000 ft (609.6 m) MSL 85°F (29.45°C) (no range credit may be taken)
6. 50 nm (92.6 km) of low-altitude, high-speed penetration
7. 2-min mid-mission Landing Zone (LZ) Hover Out of Ground Effect (HOGE) at Mid-Mission Gross Weight (MMGW).
8. Cruise-climb at best climb speed (VBROC) where range credit may be taken for the total Radius of Action (ROA) in flight legs 4 and 6
9. Cruise 450 nm (833 km) at no less than 20,000 ft (6,096 m) ISA conditions or best cruise altitude at the best range speed (V_{BR}) or no less than 450 KTAS (833 km/hr)
10. Descend to 2,000 ft (609.6 m) MSL 85°F (29.45°C) (no range credit may be taken)
11. 50 nm (92.6 km) of low-altitude, high-speed penetration
12. 2-min Hover In Ground Effect (HIGE) takeoff (close to surface, less than 1 rotor diameter). Fuel/Energy reserves shall be 20 min at VBR and 2k/85°F (609.6/29.45°C).

Takeoff Criteria

- 2k/85°F
- HIGE Takeoff
- HOGE at Mid-Mission (MMGW)
- 90% Engine MRP, 100% Const. XMSN Torque

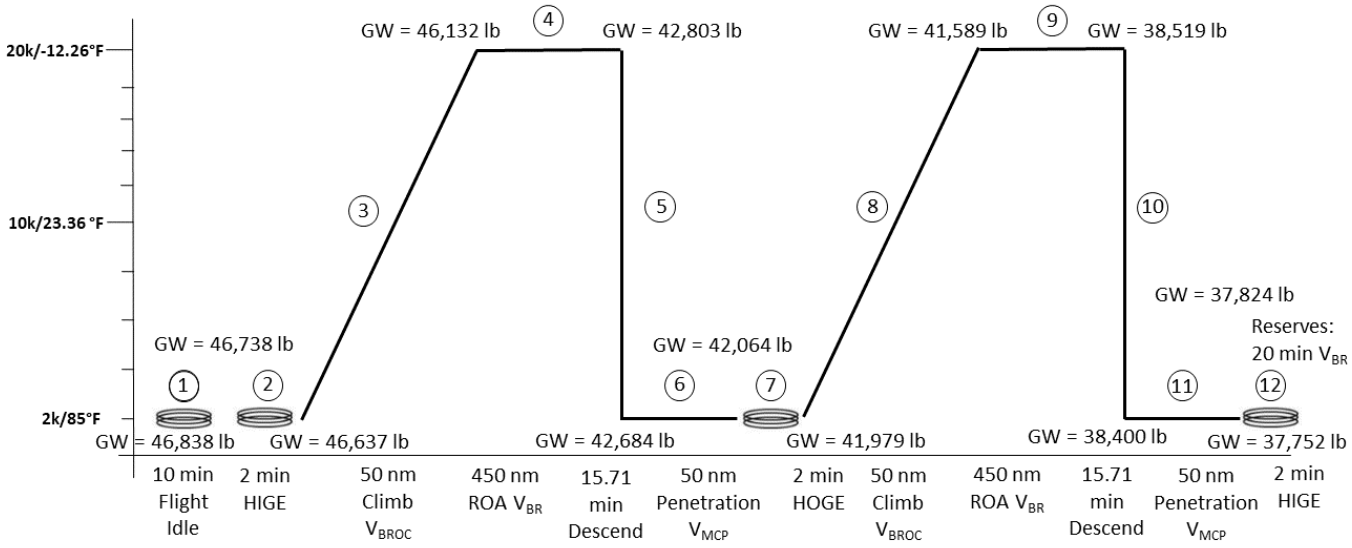

Figure 1.1: Resupply Mission Profile

2 Configuration Selection

Karfi is a thrust-compounding, two-speed transmission, transport tiltrotor designed for high speed forward flight and VTOL capabilities. A careful and rigorous configuration process was followed which took the results from the RFP analysis and converted them them into a set of criteria, (Section 2.1). These criteria were then used as a baseline when conducting trade studies into current and experimental VTOL

configurations, the process for which is detailed in Figure 2.1.

2.1 Criteria Formulation

In order to avoid bias while creating the criteria, each team member individually created a list containing all the important factors that, if met, would signify a successful design per the RFP requirements discussed in Section 1.1. Afterwards, the team regrouped, compared results and arrived at a consensus. The chosen criteria were further expanded on, including formulating definitions and quantifiable metrics for evaluation. Through this process, the number of criteria was refined from 27 to 6. The final criteria are listed below:

- **Threat Avoidance:** To effectively complete the required mission, our aircraft must "incorporate technologies and design features enabling threat avoidance to meet critical military needs in highly-contested environments" (Paragraph 1, Section 2.0). Consequently, the aircraft must incorporate stealth technologies to decrease noise, thermal signature and radar cross section.
- **High Speed Capabilities:** Per the RFP requirements and mission profile, the aircraft primarily operates at high-speed conditions, with a required 450 kts (833.4 km/h) cruise speed at 20,000 ft (6,096 m) altitude minimum requirement. As a result, this criterion focuses on evaluating a concept's characteristics under such conditions, with emphasis on the lift to drag ratio.
- **Minimization of Gross Takeoff Weight:** In order to facilitate the diametrically opposed criteria for high-speed forward flight and VTOL capabilities, it is necessary to minimize the gross takeoff weight of the vehicle; whether it be structural weight savings, lower fuel requirements, less engines, etc.
- **Technology Readiness Level:** Technology Readiness Level (TRL) balances the imagination and originality of the design with the real-world limits associated with it. The aircraft design should be novel but it should also be manufacturable. While new and innovative technologies should be explored, the design should not rely on purely hypothetical technology. If the design relies on a component that is completely unproven and untested, the design will need to be reevaluated.
- **Downwash/Outwash Effects:** The RFP is specifically looking for a vehicle capable of mitigating the downwash/outwash (Paragraph 8, Section 2.1) in order to facilitate usage in highly contested environments (unprepared surfaces) and ease of aircraft operations.
- **Life Cycle Cost:** Although certain concepts may be feasible in theory, if the life cycle cost is too high, then it may not be a realistic solution. As a result, this criterion analyzes the cost to produce, cost to maintain and cost to operate each concept in order to determine whether it can realistically be put into service.

2.2 Conceptual Design Trade Studies

The process of finding the best configuration that fit the RFP's requirements is detailed in Figure 2.1. Over ten different configurations were considered, including a baseline single main rotor (SMR) design, fan in wing, various tiltrotor designs and an X wing design. The first step was to analyze all the different designs to see which were capable of achieving the 450 kts (833.4 km/h) cruise speed. This process eliminated configurations such as the SMR and tandem rotor configuration. Afterwards, of those that seemed capable of the required speed, disk loading was investigated. The RFP requested that downwash/outwash effects be investigated and minimized for crew operations. Initial calculations were done on the configurations and it was found that, for example, a fan in wing design required a span of over 150 ft (45.72 m) to get

a reasonable disk loading around 23 lb/ft^2 (1,101.25 Pa). For the cases where the configuration required unacceptable parameters to accommodate desired disk loading, it was discarded. Finally, after this step, only three remaining configurations remained, where more detailed trade studies were done, Sections 2.2.1, 2.2.2, and 2.2.3. During this stage, other important factors were considered such as the ability to have a TRL level 9 by 2035, life cycle cost and mechanical complexity. Only one single configuration stood out as meeting all the RFP requirements, the Thrust Compounding Tiltrotor with 2-Speed Transmission, which was selected for *Karfi*.

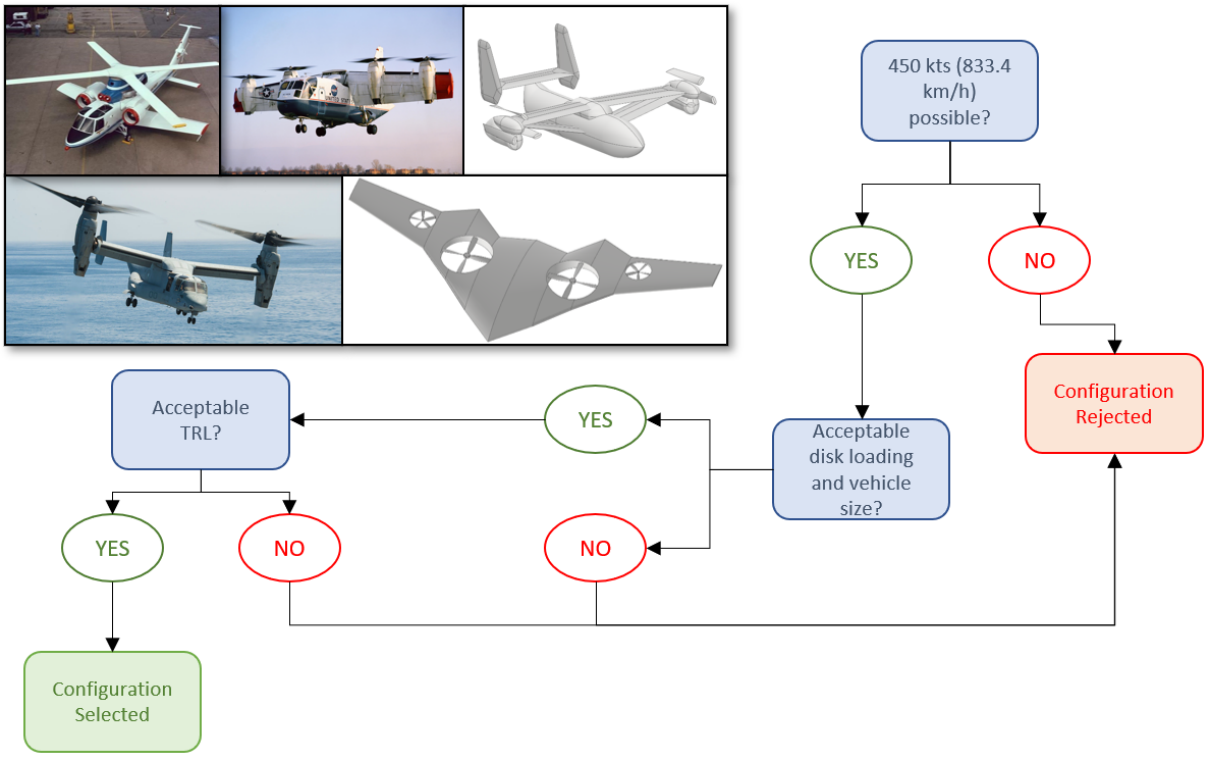

Figure 2.1: Process Flow for Configuration Selection

2.2.1 Thrust Compounded Variable Diameter Tiltrotor

The variable diameter tiltrotor configuration (VDTR) relies on a change in rotor diameter to influence the rotor tip speed and stay below the drag divergence Mach number during high-speed forward flight as well as keep the disk loading to a minimum during VTOL operations. This system relies on both the thrust produced by the rotors and a separate propulsion system to achieve the necessary speed of at least 450 kts (833.4 km/h).

However, several issues arise when trying to modify the rotors drastically during flight. Firstly, most VDTR concepts published require the use of inner telescoping mechanism where the spar can be retracted and extended to create the variable diameter. Consequently, limits must be placed on the proprotor design to allow for sufficient telescoping movement. These restrictions in turn reduce the blade efficiency during forward flight since high twist is essential for axial flight and sweep is beneficial for reducing even further the drag caused by the spinning proprotors. Additionally, it was found that the VDTR design has consequential life cycle stresses. Varying the rotor diameter can cause a strong bending moment which in turn could lead to fatigue of the spar, a component vital to the VDTR design [7]. Finally, preliminary

calculations were made for the VDTR concept and it was found, that even with a 30% decrease in rotor radius (a design limitation of the VDTR concept), to keep the rotor tip Mach at 0.85, the rotor RPM needed to be 253 RPM (an approximate 23% RPM reduction from the V-22's operating 330 RPM). As a result, the VDTR concept would not be able to stay underneath the drag divergence number in the flight conditions detailed in the RFP. Because of these reasons, the VDTR was found to not be the optimal choice for this RFP.

Figure 2.2: UMD HeliX Design [1]

Cost analysis was also taken into account when analyzing the configurations. From a report investigating the VDTR concept by Mark Scott, it was determined that the cost per pound in 2023 dollars for this configuration is $3,233 [2]. Using this factor with the weight estimate provided in the report, the total manufacturing cost for the VDTR is $128.803 M.

2.2.2 Thrust-Compounding Foldable Tiltrotor

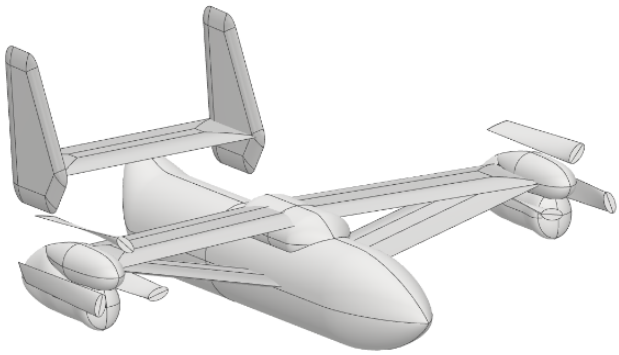

Figure 2.3: Initial Design for Foldable Tiltrotor

The foldable tiltrotor (FTR) concept proved most interesting in how it dealt with the drag created by

an open rotor system in high-speed forward flight. To avoid exceeding the drag divergence Mach number ($M_D = 0.85$ for the designed cruise conditions), this design takes the rotor system away entirely. Because of this, the rotors can be designed mainly for hover efficiency. Additionally, with the rotor blades folded back, the vehicle's radar cross section is minimized, leading to enhanced threat avoidance.

On the other hand, several key disadvantages appear in this configuration which disqualified this configuration as a final solution. Firstly, in order to provide both VTOL capabilities and high-speed forward flight during the same mission, the rotors must be folded and redeployed during flight. This will require a robust, and very heavy mechanism for both stopping the rotors in flight and then folding them. Furthermore, for the proposed mission profile, this vehicle would be required to fold and redeploy its rotor system a total of 4 times per mission which would have important consequences on the life cycle of the rotor hub and vehicle. Additionally, during high-speed forward flight, the main flight condition for the design mission profile, the folded rotors provide no value to the vehicle, serving mainly as dead weight. Moreover, even when folded, the rotors are exposed to the freestream, increasing the drag around the nacelle of the vehicle. The rotor hub system is also required to be larger than that of a traditional tiltrotor to house the folding mechanism as well as the braking mechanism necessary to stop the rotors in flight, which again increases the drag area. The added complexity as well as more demanding life cycle leads to more potential weak points in the design. Lastly, while the foldable tiltrotor design has been under development by Bell for some time now, they most recently confirmed a TRL 4 after a 2021 test [8]. This means that there is a very low chance that the technology will be able to reach TRL 9 by 2035. Because of all these reasons, the foldable tiltrotor with thrust compounding was not chosen as a solution to satisfy the RFP requirements.

For the cost analysis of this configuration, it was assumed that the cost per pound for an FTR concept in 2023 is equal to that of the VDTR design due to the similar TRL level. Using a report published by Wilkerson, it was determined that the total manufacturing cost for a foldable tiltrotor conceot in 2023 is $173.295 M.

2.2.3 Thrust Compounding Tiltrotor with 2-Speed Transmission

Unlike the previous tiltrotor designs covered, this concept does not modify the rotors in any way to enable efficient high-speed forward flight; instead, it utilizes a two-speed transmission to reduce the rotor RPM by 50% to reduce the drag in this flight condition. Additionally, this unique decision allows for increased freedom in terms of proprotor design, allowing for tip sweep and high twist. From calculations, it was found that to keep the proprotor tip Mach number below 0.85 at 20,000 ft, a 50% reduction in rotor RPM was more than enough, especially with a rotor taper. Furthermore, unlike the previous two designs, the novel technology on this configuration is housed within the nacelle, away from the strong aerodynamic forces the proprotor hub is subject to, leading to a higher life cycle.

In 1953 an Air Force H-5H helicopter test flew a two-speed transmission, [9] that functioned similarly to *Karfi*'s, maintaining a constant engine speed while varying the proprotor speed. The flight tests showed that the two-speed transmission offered significant advantages, most notaby decreasing proprotor tip speed. Additionally, Karem Aircraft Incorporated, an independent aerospace company, has successfully performed a full scale test of the two-speed transmission system at both operating conditions while Boeing, with its A160 Hummingbird, has also provided a flying example of a helicopter with a two-speed transmission [[10], [11]]. As a result, if continued support for this technology is maintained, it could easily reach TRL level 9 by the required year of 2035. The main disadvantages of this concept in comparison to the previous two is that there are still large open rotors in high speed forward flight which increases the risk of whirl flutter, and there is no reduction of radar cross sectional area. Because of the advantages mentioned above, this configuration was selected as the most suitable solution for the RFP requirements.

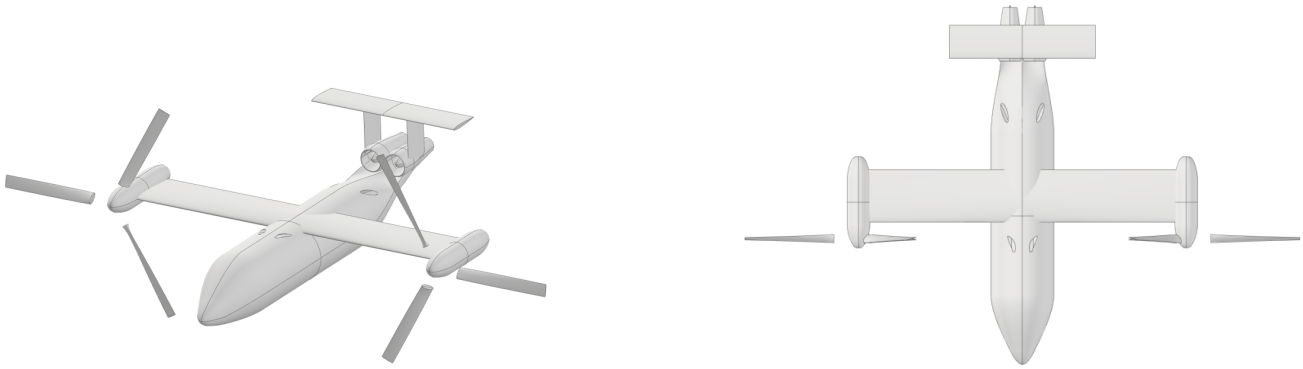

Figure 2.4: Two Speed Transmission Tiltrotor with Compound Propulsion

A cost study was done for this configuration using NASA's Design and Analysis of Rotorcraft (NDARC), of which a more detailed description is provided in Section 10. It was found that the manufacturing cost for a thrust compounding tiltrotor with two-speed transmission is approximately $154.484 M, in between the previous two designs. The full cost analysis and results are detailed in Section 10.

3 Vehicle Trade Studies and Sizing

In order to determine *Karfi*'s key characteristics, parametric trade studies were performed on vehicle components/attributes in order to optimize the vehicle performance. This included vehicle sizing investigations using blade momentum theory (BMT) and blade element momentum theory (BEMT). The results of the investigations are detailed in Table 3.1.

Parameter	**Thrust-Compounded Two-Speed Tiltrotor**
SDGW **[lb]** (kg)	**46,828** (21,241)
Empty Weight **[lb]** (kg)	**29,374** (13,324)
Total Fuel Weight **[lb]** (kg)	**10,235** (4,644.69)
Proprotor Radius **[ft]** (m)	**20.67** (6.3)
Number of Blades	**3**
Disk Loading **[lb/ft^3]** (Pa)	**19.5** (47.88)
V_{tip} in Hover **[ft/s]** (m/s)	**750** (228.6)
V_{tip} in Cruise **[ft/s]** (m/s)	**375** (114.3)
Solidity	**0.1**
Wing Span **[ft]** (m)	**57.33** (17.47)
Wing Chord **[ft]** (m)	**9.56** (2.91)
Installed Turboshaft Power **[hp]** (kW)	**2x5,476** (2x4,083.1)
Installed Turbofan Thrust **[lb]** (N)	**2x7,210** (2x32,072)

Table 3.1: *Karfi* Vehicle Parameters

3.1 Sizing Code Methodology

The team developed an in-house sizing code, see flowchart in Figure 3.1, using modified BMT and BEMT to model the vehicle's dynamics in hover, climb, cruise and descent. Sizing begins with an initial

estimation of gross takeoff weight, and mission requirements such as payload, altitude and cruise speed. Then, drag and power calculations were carried out segment by segment, corresponding to the various mission profile steps. This process automatically iterates itself until mass converges and final numbers are found.

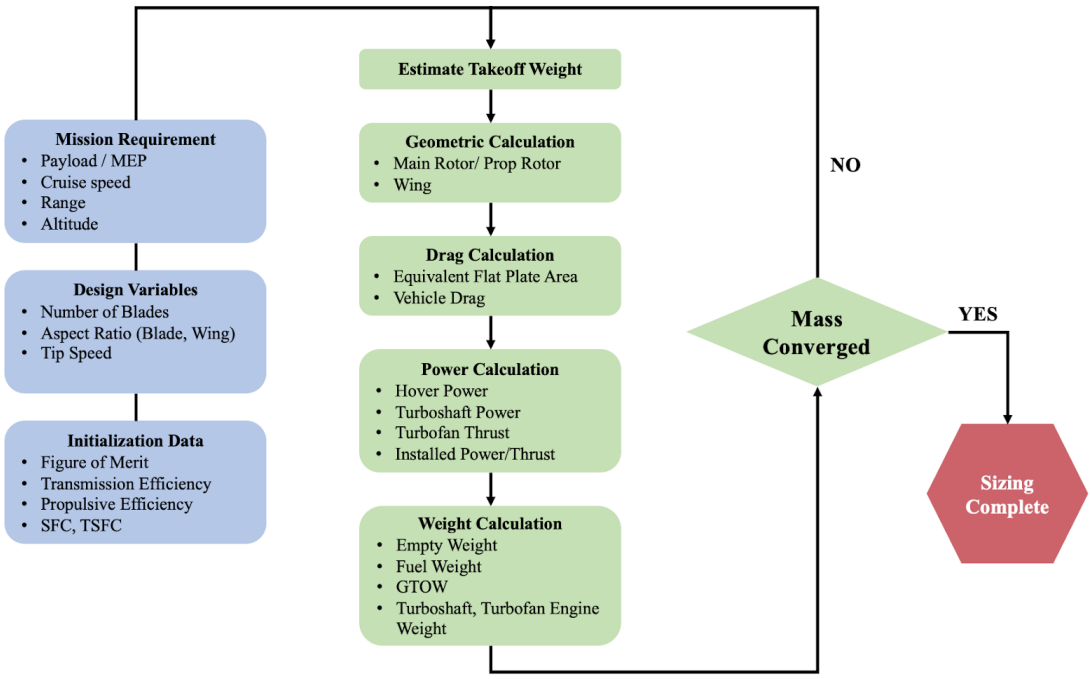

Figure 3.1: Flowchart of Vehicle Sizing Code Procedure

The process and equations used to build the vehicle component weights were based on statistical approximations, the U.S. Army's Aeroflightdynamics Directorate (AFDD) and NASA Design and Analysis of Rotorcraft (NDARC) [12], [13], [14]. The mission profile was decomposed into segments, and the power required and fuel consumed were calculated for each.

3.1.1 Sizing Code Drag Estimation

In forward flight, the power required to cruise at 450 kts (833.4 km/h) is equivalent to the product of drag and velocity. Hence, drag estimation was a critical component in the sizing code setup. First, the equivalent flat plate area of the aircraft was calculated using Equation 1 where GTOW is in lb and K is a scaling factor, 1.5 in this case. Next, Equation 2 [15] was used to estimate parasitic drag, where q is dynamic pressure.

$$f = K(\frac{GTOW}{1,000})^{2/3} \tag{1}$$

$$D = qf \tag{2}$$

3.1.2 Sizing Code Altitude Effects on Turboshaft Engine Power

The mission profile requires the vehicle to cruise at no less than 20,000 ft (6,096 m) for a total of 900 (1,666.8 km) out of the 1,000 nm (1,852 km) mission distance. As a result, the aircraft's main operational environment is at high altitude and thus the power installation losses must be taken into account, equation 3 [16], where θ is the temperature ratio at altitude and δ is the pressure ratio at altitude.

$$P(\theta, \delta, M) = P(1, 1, 0)[(1 - KT(\theta - 1))(1 + KD(\delta - 1))] \tag{3}$$

3.2 Sizing Code Validation

The cruise performance code was validated against Scott's high speed tilitrotor analysis, [2]. This data was used to validate the in-house sizing code built by the team. Specifically, the disk loading (20 lb/ft^2 (957.6 Pa)) and gross takeoff weight (39,839 lb (18,070.67 kg)) reported by Scott were used as inputs [2]. Figure 3.2 demonstrates good correlation between the code and the results [2] except above 400 kts (740.8 km/h) where the present code underestimates the power required by about 8.5%.

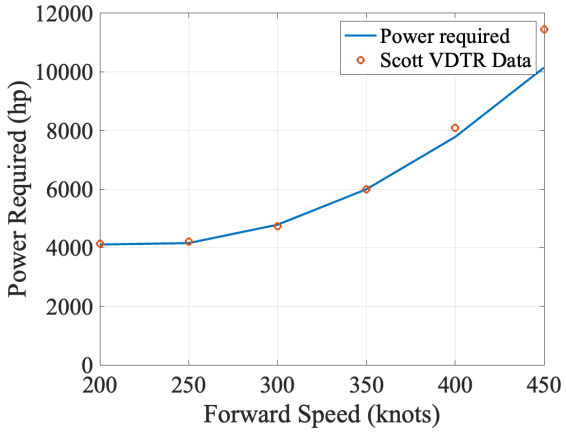

Figure 3.2: Airplane Mode Code Validation at a Cruise Altitude of 20,000 ft [2]

3.3 Vehicle Parameter Trade Studies

3.3.1 Disk Loading

According to the RFP, disk loading is an important parameter when it comes to identifying a VTOL aircraft's ability to handle unprepared surfaces. For example, an aircraft with a disk loading of above 40 lb/ft^2 (1,915.2 Pa) is only capable of VTOL maneuvers on tarmac while an aircraft with a disk loading less than 6 lb/ft^2 (287.28 Pa) is able to handle most surfaces including dry sand with minor surface degradation.

Disk loading was optimized for best performance with consideration to the effects of downwash and outwash on the takeoff and landing environment.

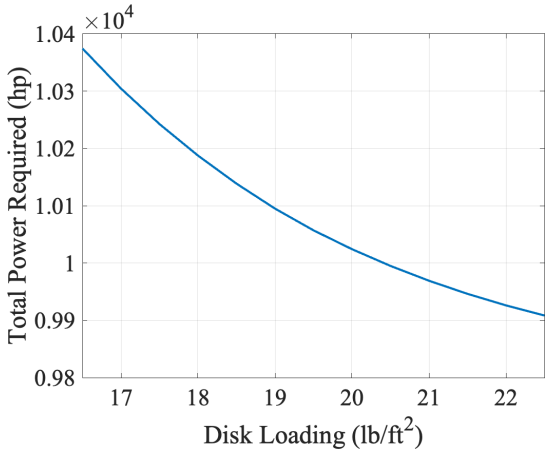

Figure 3.3: Total Power Required vs Disk Loading

Figure 3.3 demonstrates the power requirements as disk loading varies. Knowing the damaging effects of high disk loading on unprepared surfaces [17], a balance between power and downwash/outwash effects can be made. A disk loading of 19.5 lb/ft^2 (933.67 Pa) was selected for *Karfi* in order to maximize the power benefits while also maintaining the ability to operate in almost any condition; such as a water rescue mission.

3.3.2 Empty Weight

With advances in isotruss structural technologies, reducing the empty weight of the aircraft was a major area where improvements could be made [18].

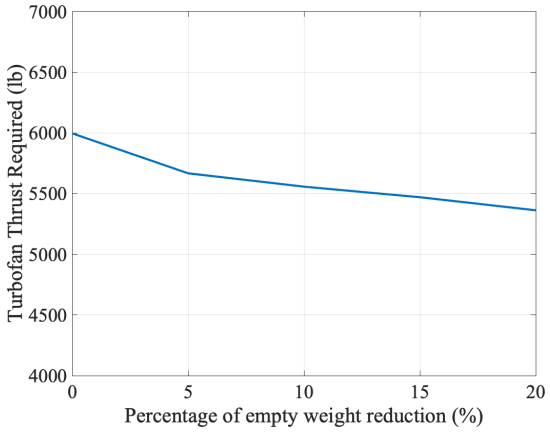

Figure 3.4: Turbofan Thrust Required vs Empty Weight Reduction

Not only does a reduction in empty weight inherently decrease the structural design gross takeoff weight of the aircraft but it also decreases the turbofan thrust required, as seen in Figure 3.4. Consequently, a 15% reduction in empty weight allows the turbofan required thrust to be decreased by 10% which in turn decreases the turbofan size and fuel required to complete the mission.

3.3.3 Proprotor Aerodynamic Properties

In the tiltrotor system, the blades act both as rotors during VTOL operations and as propellers during forward flight. Consequently, it was important to optimize the design of the blades for highest efficiency in both flight regimes.

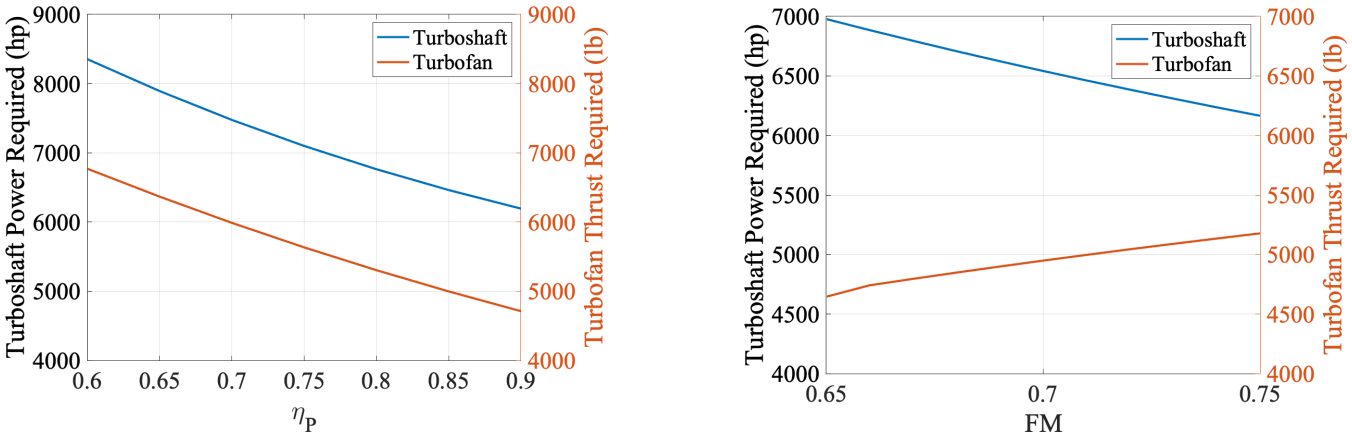

Figure 3.5: Parametric Trade Study on Rotor Aerodynamic Properties

From the results in Figure 3.5, optimizing the Figure of Merit of the proprotor blade results in higher efficiency gains for a high speed tiltrotor design rather than designing for the best propeller efficiency. For these reasons, *Karfi* was designed to have a figure of merit of 0.85 while having a propeller efficiency of 0.51.

3.4 Engine Trade Studies

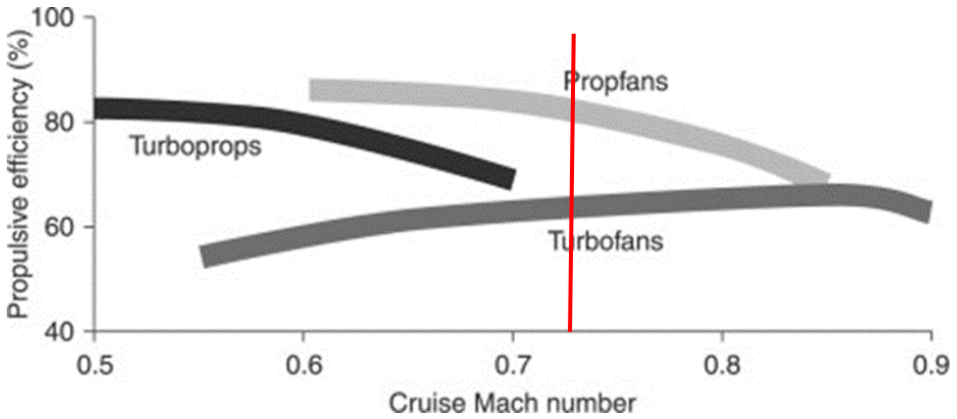

Figure 3.6: Propulsive Efficiency vs Mach for Turbine Engines [3]

The chosen design for *Karfi*, that of a tiltrotor with a two-speed transmission, requires the use of a compound propulsion system in order to achieve the desired cruise speed of 450 kts (833.4 km/h). Several different options were considered. Piston engines were quickly eliminated from contention because of their

lower power to weight ratio and trouble with having sufficient airflow at high altitudes, such as 20,000 ft (6,096 m). Electric propulsion systems reliant on batteries were also ruled out due to the range requirement of the mission profile, a total of 1,000 nm (1,852 km), which would require batteris of such high weight and volume, infeasible for airborne vehicles.

For the designed cruise conditions (Mach number = 0.73), propfans are the most efficient, see Figure 3.6. However, propfans pose several serious limitations. Firstly, they impose strict geometric requirements for their placement due to the open blade design. The exposed fans cannot be hidden away in a fuselage or be mounted near other aerodynamic surfaces as they require clean airflow to be efficient. Additionally, these exposed fans would also help to increase the vehicles radar cross section, a characteristic of the vehicle that should be minimized for enhanced threat avoidance. Therefore, turbofan engines were selected as the complementary propulsion system.

Figure 3.7: Propfan Engine [4]

In the 1970s and 80s the US government was heavily interested in high-speed rotorcraft. This interest resulted in substantial funding for research projects that could lead to a high speed, VTOL capable vehicle. One area that received massive funding was the idea of a convertible engine, a gas turbine engine that could provide both shaft power for a rotor and jet thrust for forward flight. The concept was heavily developed by both NASA and Pratt & Whitney, however, convertible engines have not been used in any aircraft despite the confidence shown in the studies. It was decided that convertible engines would not be used in this design because they are considered too risky an innovation to be sure of implementation by 2035. A convertible engine would be an elegant solution to the design challenges that a VTOL aircraft flying at 450 kts (833.4 km/h) creates, but the technology is not mature enough to implement on an aircraft entering service by 2035. As a result, the choice was made to utilize a combination of traditional turboshaft and turbofan engines.

4 Proprotor and Wing Design

4.1 Proprotor System Design

The Proprotor system is designed to provide the thrust needed for helicopter flight mode while maintaining a low disk loading to minimize downwash and outwash effects on the ground personnel. The system utilizes a three-bladed, gimballed rotor hub that helps reduce the moments and forces transmitted to the airframe.

4.1.1 Proprotor Aerodynamic Design

The rotor aerodynamic design was performed with an in-house propeller code that uses Blade Element Momentum Theory (BEMT) for both hover and axial cruise flight. Unlike a typical single main rotor design, *Karfi* tilts its proprotor system 90° during forward flight, allowing the turboshaft engines to supplement forward thrust. As a result, both Figure of Merit (FM) and propeller efficiency (η_P) were calculated using methods in [19].

The code was validated against the University of Maryland's past VFS SDC design, *Excalibur*. For the proprotor blade design, the geometric choices made were to maximize proprotor efficiency in hover. Although cruise is the main operating condition for *Karfi*, as seen in section 3.3.3, figure of merit had the biggest impact on turboshaft engine efficiency.

Several airfoils were considered, including the RC4-10, RC3-8, Clark-Y, MH-60, and Clark-YH. The RC3-8 airfoil was chosen due to its low t/c ratio (8%) with the intent to reduce the drag and weight of the system. For manufacturing simplicity, the airfoil was kept constant throughout the blade.

Twist angle, taper ratio, and taper transition point also varied during the study.

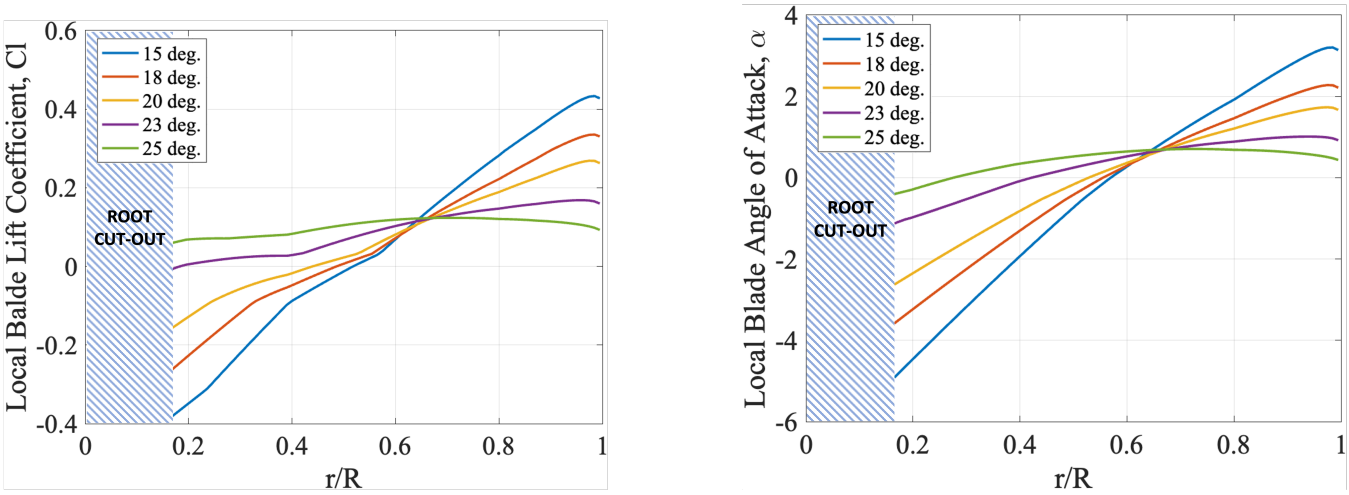

Figure 4.1: Proprotor Twist Angle Study in Hover

The twist angle study (all twist angles are negative) demonstrated that for twist angles equal or less than 20°, the blade produces negative lift close until approximately 50% of the blade's span. Additionally, a twist angle of 25° gives approximately a uniform local blade angle of attack across the span; however, due to differential flow across the blade, this is not ideal. For these reasons, a twist angle of 23° was chosen.

For the other parameters, a taper ratio of 2:1 and a taper transition point at 80% span was chosen. The final specifications for the proprotor design are tabulated in table 4.1 below.

Parameter	**Value**
Number of Blades	**3**
Aspect Ratio	**9.55**
Radius **[lb]** (kg)	**20.67** (6.3)
Solidity	**0.1**
FM in Hover	**0.85**
η_P in Cruise	**0.51**
Tip Speed in Hover **[ft/s]** (m/s)	**750** (228.6)
Tip Speed in Cruise **[ft/s]** (m/s)	**375** (114.3)
C_T/σ in Hover	**0.1596**
C_T/σ in Cruise	**0.042**

Table 4.1: *Karfi* Proprotor Specifications

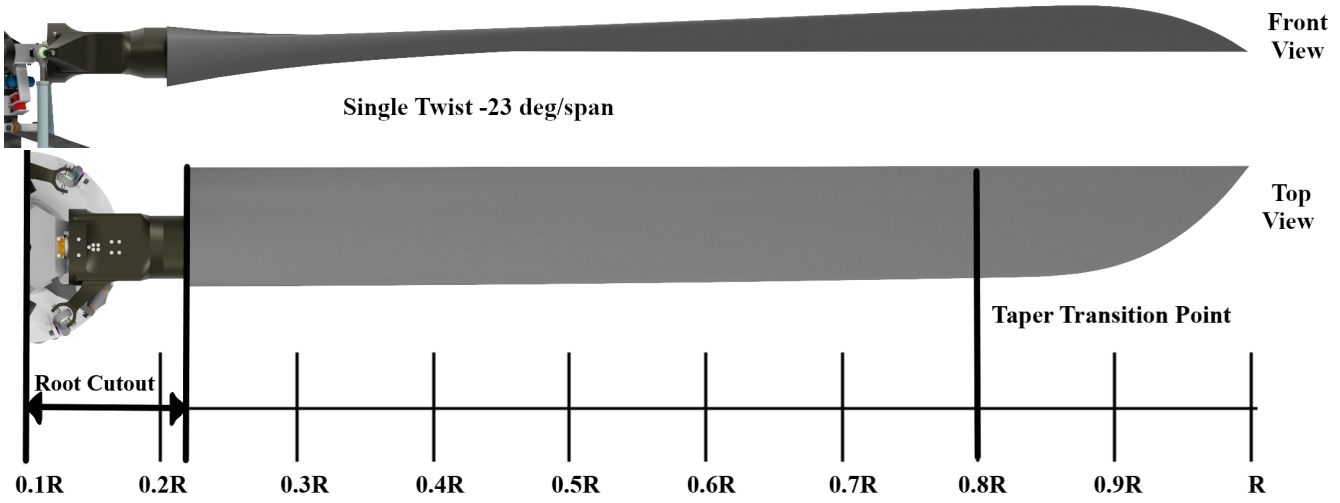

Figure 4.2: Proprotor Geometry

4.1.2 Rotor Structural Design

The structure of the proprotor blade is designed to resist lead-lag, flap, and torsional moments in addition to the centrifugal forces and shear stresses that the blade will experience during flight [15]. The composite D-spar and trailing edge block are the primary load bearing members and provide flap, lead-lag, axial and torsional stiffness. Aft of the D-spar is Nomex Honeycomb to maintain the aerodynamic profile of the blade and provide stiffness. To maintain the center of gravity at the quarter chord, tungsten alloy leading edge weights are employed for their high density that minimizes the space taken up within the blade structure.

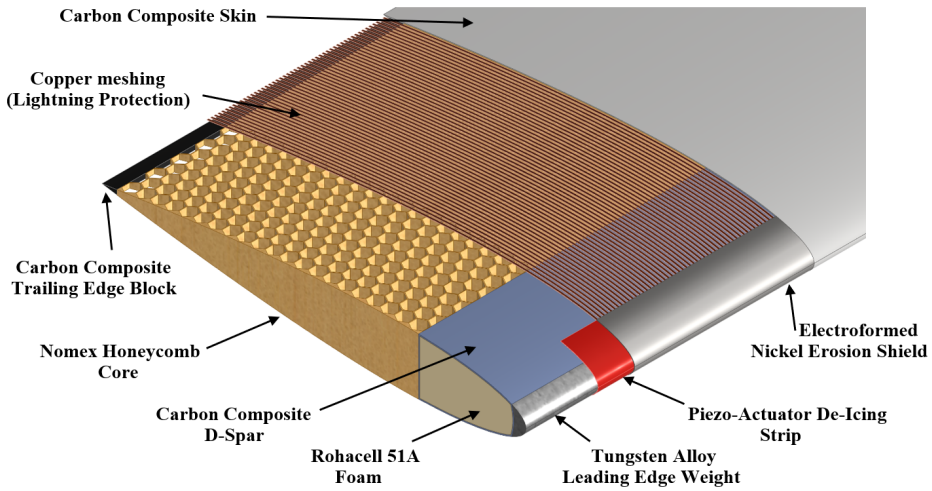

Figure 4.3: Blade Structural Composition

The blade skin is composed of two carbon composite fabric layers in a $\pm$ 45° layup [15]. De-icing is provided with a piezo-actuator layer at the leading edge of the blade. Electro-thermal de-icing methods were considered but not chosen for their additional power consumption and weight over a piezo-actuator

system. The erosion shield is composed of electroformed nickel with polyurethane tape over it for easy to repair erosion protection. Lightning protection is provided by copper meshing embedded into the skin of the blade, allowing for the electrical energy to be transmitted to a ground point.

4.2 Rotor Hub Design

The main proprotor hub assembly is a critical sub-system of *Karfi*'s propulsion system. The proprotor hub provides the connection between the mast and the rotor, transfers the blade loads from the rotating frame to the fixed frame, transfers the torque to the rotor, and transmits blade control. These functions must be performed while maintaining a low weight, low drag, mechanical simplicity, low part count, low cost, and long fatigue life. A carefully designed hub is crucial for *Karfi*'s ability to achieve the RFP's requirements.

4.2.1 Gimballed Hub

Gimballed Hubs use an elastically tailored yoke to provide a virtual coning hinge, along with a constant velocity (CV) joint to provide the range of motion for the gimbal action and to ensure that the yoke and rotor shaft are operating at the same speed. The CV joint allows gimballed hubs to not transmit the moments produced by the rotor to the rest of the aircraft.

In addition, gimballed hubs also provide relief for the one-per-rev blade flapping loads while severely reducing the blade acceleration and deceleration induced by blade flapping, due to the hub's ability to rotate [15]. Due to their compact size and reduction of transmitted moments and loads to the airframe, gimballed hubs were selected for the design.

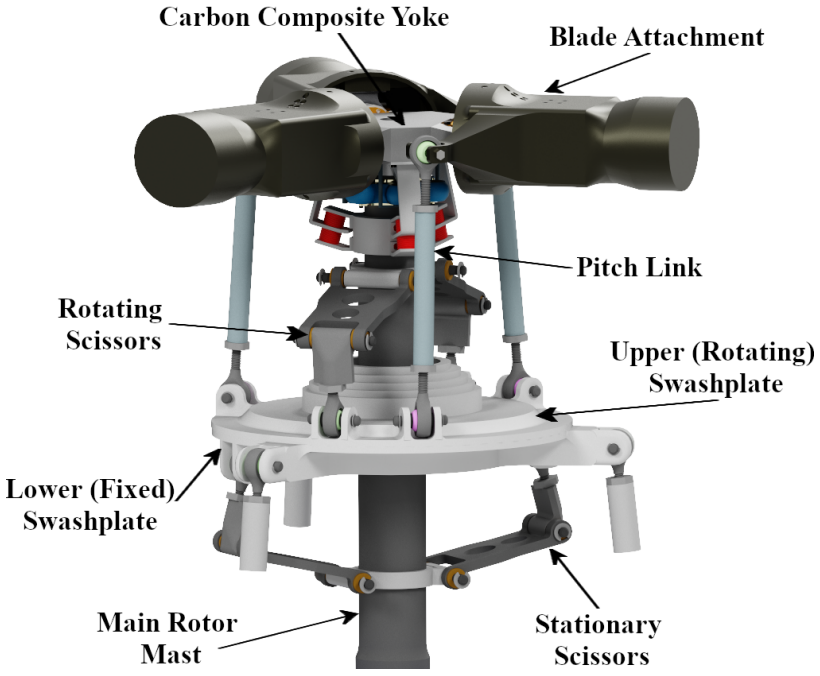

Figure 4.4: *Karfi*'s Gimballed Rotor Hub

The forces produced by the blades are transferred via a blade clamp to a collection of bearings. These bearings are sandwiched between the yoke on both sides. The side further away from the hub contains

a conical elastomeric bearing. This conical bearing's inboard face links with a blade clamp, while the outboard face connects to a thrust bearing. Due to the rotation of the blades, the conical bearing is always under compression, dealing with the centrifugal forces and flap and lag shear forces generated between the blades and the yoke [15].

4.2.2 Bearing Assembly

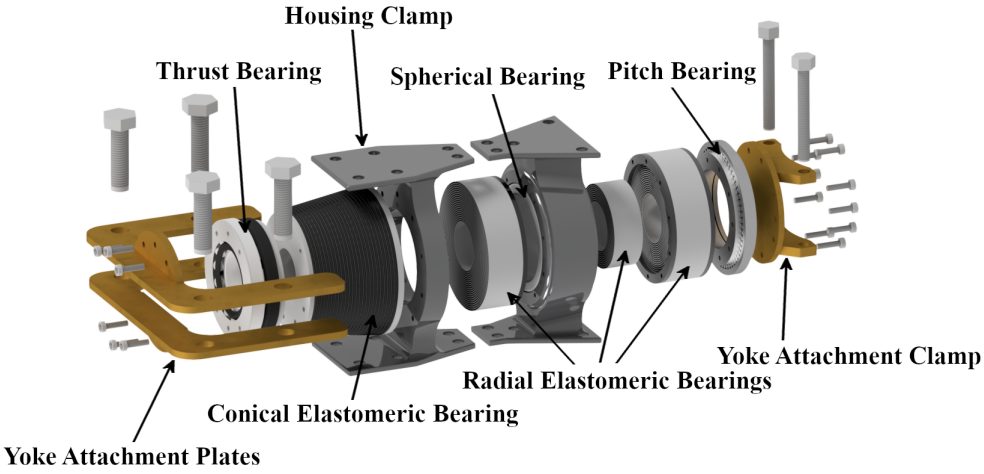

Figure 4.5: Bearing assembly (Exploded View)

The inboard assembly is a tightly-knit arrangement of three radial elastomeric bearings and a spherical elastomeric bearing. All the radial bearings are aligned in parallel with the central one housed within the spherical bearing. This spherical bearing is in turn secured to the pitch housing by a clamp. This smart design enables rotational forces from the pitch housing to be distributed to all the bearings [20], allowing a broad pitch range.

The bearing assembly's innermost part comprises the pitch bearing and solenoid, essential for the wide range of blade pitch adjustments required by the aircraft design. A solenoid limits the pitch bearing and the proprotor blades' rotation, locking them into the appropriate orientation for helicopter or forward flight modes via radial slots located on the inner face of the bearing. The slots are located 55° apart, allowing for the ideal blade pitch setting determined in our aerodynamic analysis for both hover and forward flight modes. To support the pitch bearing during the rotation of the assembly, a spherical roller thrust bearing is mounted at the most outboard portion of the assembly to help share the axial and radial loads. This system provides the large pitch setting range needed for the assembly to achieve efficient flight performance in both hover and forward flight without sacrificing performance in either flight mode.

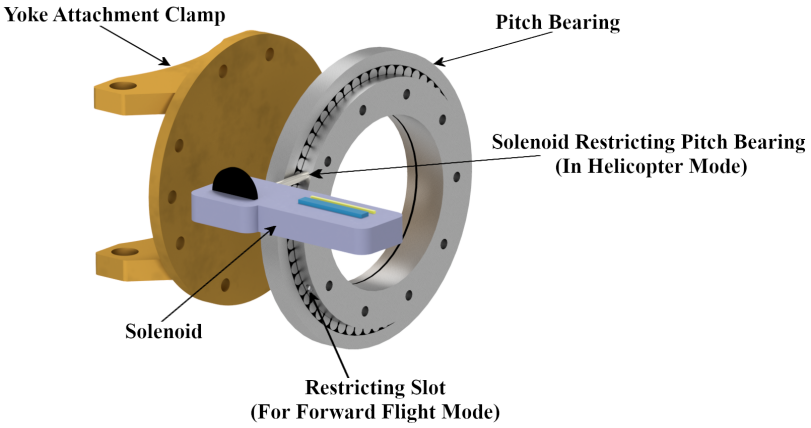

Figure 4.6: Pitch Bearing and Solenoid Assembly

4.2.3 Constant Velocity Joint and Hub Springs

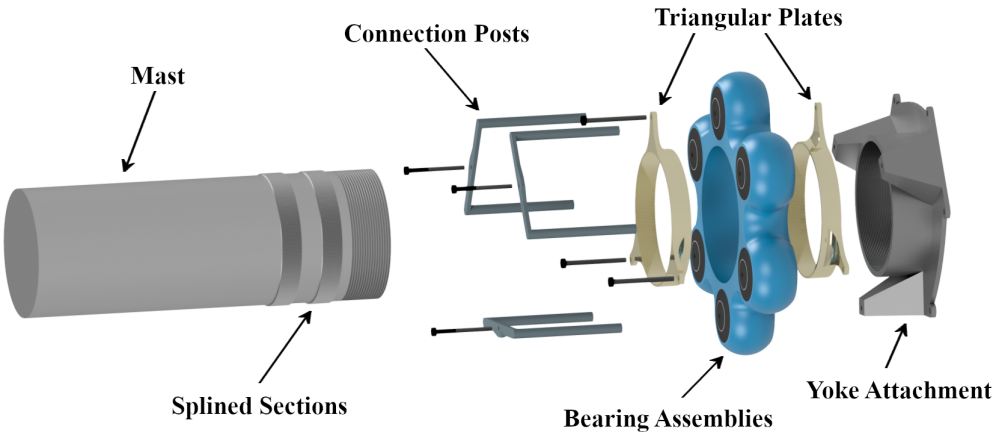

Figure 4.7: Constant Velocity Joint (Exploded View)

Given the flexible (gimballed) nature of the hub, the hub's axis can tilt relative to the shaft's axis. To avoid any speed discrepancies between the hub and rotor shaft due to this potential misalignment, a constant velocity joint is employed. Without this joint, misalignment could induce a two-per-revolution oscillation, causing disruptive vibrations and potentially leading to whirl flutter instabilities [15]. The constant velocity joint is crafted from six elastomeric bearing assembly, granting the required degrees of freedom for gimbal functions. It's held secure to the mast through specially designed plates.

Three external hub elastomeric bearings, housed within U-shaped posts, link the yoke to the mast. These compressed bearings function as hub springs, reducing angular misalignment between the yoke and the mast, while aiding in transferring thrust loads from the proprotor blades.

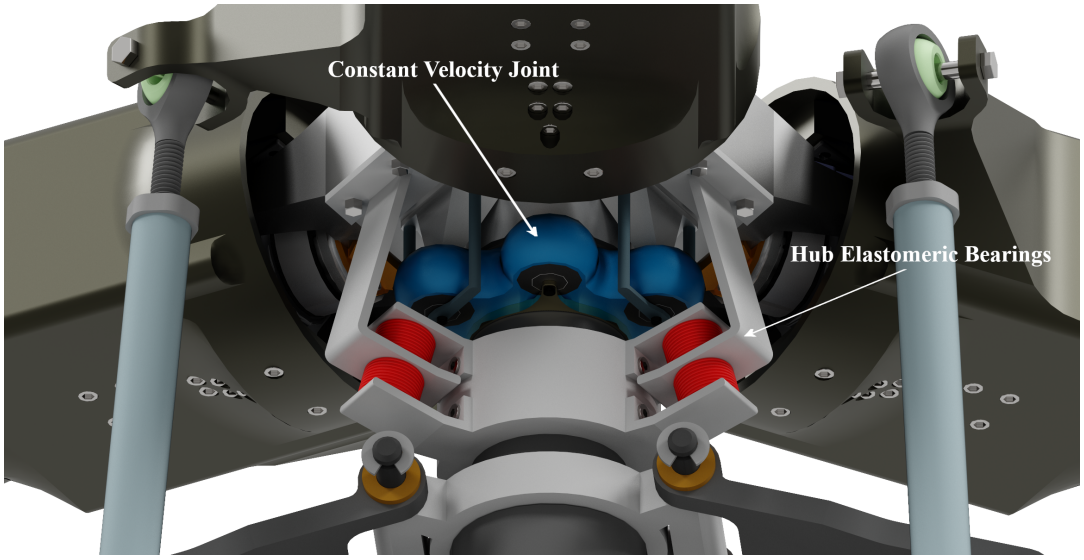

Figure 4.8: Gimbal and CV Joint Assembly

4.2.4 Rotor Yoke

The Hub employs a composite yoke, engineered to function as a virtual flap and lag hinge. This design decision eliminates the need for traditional mechanical hinges, reducing the hub's size and complexity. It also contributes to a compact and aerodynamically efficient design.

4.3 Nacelle Design

Unlike a typical design, Karfi's nacelle is area ruled. This curvature adjustment effectively reduces the airflow speed over the rotor blades, successfully averting potential transonic effects that can arise in conventional fairing designs especially with the target speed freestream at M = 0.72 which could accelerate above M = 0.75 along a conventional fairing, Figure 8.2. This alteration results in a smoother hub-to-blade transition, ensuring continuous subsonic airflow. Consequently, it effectively addresses the detrimental effects associated with transonic flow on rotor blades, such as heightened drag, diminished lift, and detrimental structural vibrations. Additionally, it prevents flow separation, which can disrupt aerodynamic forces and compromise stability. Moreover, this modification minimizes buffeting effects, thereby bolstering the proprotor system's overall performance, efficiency, and safety. Simultaneously, it safeguards the long-term durability and structural integrity of the blades.

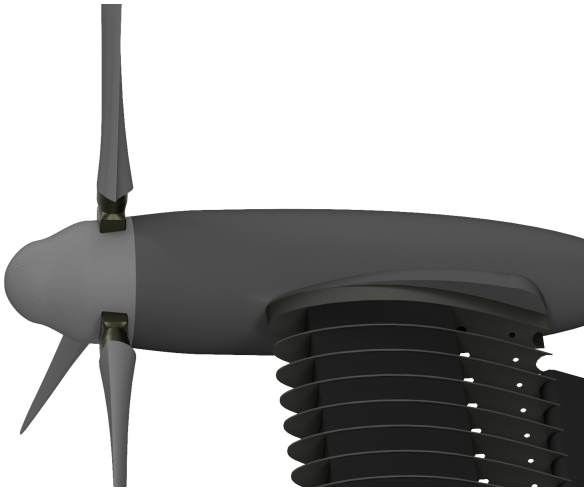

Figure 4.9: Nacelle Aerodynamic Design

Since the turboshaft engines are located in the fuselage, the nacelles are much lighter than a standard tiltrotor. The entire nacelle rotates without a large weight addition because of its relatively light weight. The nacelle is tilted using a linear actuator on a 3-bar mechanism similar to the XV-15 and V-22. The actuator is connected to an actuator spindle that allows the linear force to result in rotation relative to the wing. The nacelle is mounted to the wing on a spindle that holds it in place while allowing it to rotate with respect to the wing.

4.4 Wing Design

4.4.1 Wing Geometry

Karfi features a top fuselage mounted wing to give clearance for nacelle rotation and Foreign Object

Debris Ingestion (FOD). The wing has a wingspan of 57.33 ft (17.47 m) with an aspect ratio of 6, where the former was an output of the sizing code and the latter was an input. A straight wing with no sweep or taper was chosen for the aircraft since it allows for a higher aspect ratio, and a better lift-to-drag ratio. A straight wing is also easier to manufacture, allows for the rotors to be connected via driveshaft to keep them spinning at the exact same rate, and allows for redundancy in case of engine failure. The wing is mounted at a 4° angle of incidence to allow for a level fuselage in trimmed cruise.

Parameter	**Value**
Wing Span **[ft]** (m)	**57.33** (17.47)
Wing Chord **[ft]** (m)	**9.56** (2.91)
Aspect Ratio	**6**
Sweep	**0°**
Taper Ratio	**1**
Vertical Position on Fuselage	**High-Wing**
Horizontal Position of Aerodynamic Center from Nose **[ft]** (m)	**28.92** (8.8 m)
Angle of Incidence	**4°**

Table 4.2: Wing Geometry

4.4.2 Airfoil Selection

The wing's main purpose in a tiltrotor is to provide sufficient lift during cruise at higher speeds. Consequently, the desired airfoil must have a very good lift-to-drag ratio since the wings carry the majority of the total load in forward flight. Additionally, an airfoil with low drag would be favorable in reducing the propulsive power needed to cruise at 450 kts (833.4 km/h). With this in mind, several airfoils were considered; ultimately, the NACA 64(3)-618 was chosen as the airfoil for *Karfi*'s wing for the following reasons: this airfoil has a low thickness for a tiltrotor, 17.9% t/c, which helps reduce drag at high speeds. and at the required range of Reynolds number (approximately 400,000), the airfoil has a reasonably high maximum lift coefficient ($C_{l,max} = 1.36$) and high lift-to-drag ratio ($(C_l/C_d)_{max} = 106.17$).

4.4.3 Wing Structural Design

Whirl Unlike typical aircraft, tiltrotors require additional wing stiffness due to the potential onset of whirl flutter. The wing houses a torque box supplemented by ribs to provide additional stiffness, as well as to provide support for the flaperon system and ensure the airfoil shape is kept. The torque box was scaled from XV-15 data, [21], to meet the RFP requirements using scaling ratios provided by Chappell [21]. This resulted in required beam bending, chord bending, and torsional stiffness values as found in Table 4.3. Based on this, the torque box was designed to have vertical webs at 5% and 50% of the aircraft's wing chord, connected by upper and lower skins. Having a closed thin wall section such as the one described allows an increase in torsional stiffness of the wing.

Stifness	Beam Bending **[lb-in^2]** (kg-m^2)	Chord Bending **[lb-in^2]** (kg-m^2)	Torsional **[lb-in^2]** (kg-m^2)
	9.35*10^9 (2.736*10^6)	**2.83*10^{10}** (8.281*10^6)	**6.09*10^9** (1.782*10^6)

Table 4.3: Torque Box Material Selection

To meet the stiffness requirements of the wing, while maintaining a 17.9% t/c and without incurring a large weight penalty, the structural members of the wing were designed with composite materials. The

use of composite materials was found to achieve a 30.5% reduction in weight relative to aerospace grade aluminum alloy while still meeting all of the structural and stiffness requirements of the wing. The torque box will be constructed out of 68 layers of T300/5208 graphite-epoxy with 73.5% ±45° plies and 26.5% 0° plies. This gives results in a torque box wall thickness of 0.348 in ($8.84*10^{-3}$ m).

Material	Density **[lb/ft^3]** (kg/m^3)	Torque Box Mass **[lbs]** (kg)	% Reduction
Aluminium	**172.9** (2,7772.1)	**2,876** (1,305.2)	**N/A**
Graphite-Epoxy	**112.4** (1,800.3)	**1,999** (906.63)	**30.5%**

Table 4.4: Torque Box Material Selection

The aircraft's fuel tanks are stored within the wing's torque box. The fuel tanks will be able to store a combined volume of 2,292 gallons (8,676.16 liters) of fuel, equivalent to 14,824 lb (6,724.05 kg), 44% more than the required 10,235 lb (4,642.5 kg) of fuel necessary to complete the mission. The fuel tanks are sectioned in order to avoid fuel sloshing affecting the aircraft's lateral center of gravity. The ribs of the wing have cutouts to house the drive shaft, synchronizing shaft, electrical wiring, and hydraulic lines.

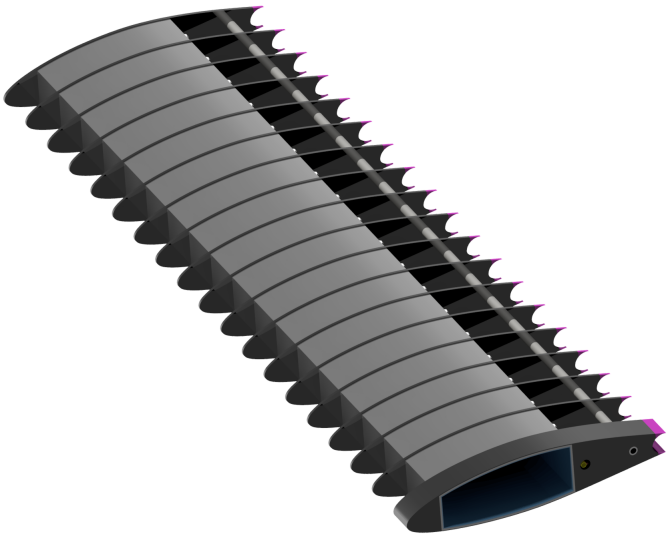

Figure 4.10: *Karfi* Wing Structure

Due to *Karfi*'s use of composite materials which are poor conductors of electricity, it is necessary that measures are taken to prevent damage to the aircraft in the case of a lightning strike. With this in mind, a copper mesh is applied to the outermost ply of the wing. An aluminum mesh was ruled out due to the likelihood of galvanic corrosion between the materials. The copper mesh will add 0.04 lb/ft^2 (1.92 Pa) of weight to the required surfaces.

4.4.4 Control Surfaces

Karfi uses a flaperon system instead of the flap-aileron system seen on most airplanes. The flaperons take up the aft 25% of the wing chord and span the middle 20 ft (6.096 m) on each wing. The flaperon

system functions as ailerons in forward flight and can be lowered symmetrically to generate a higher lift coefficient in the same way as flaps. The system is actuated by a hydraulic system.

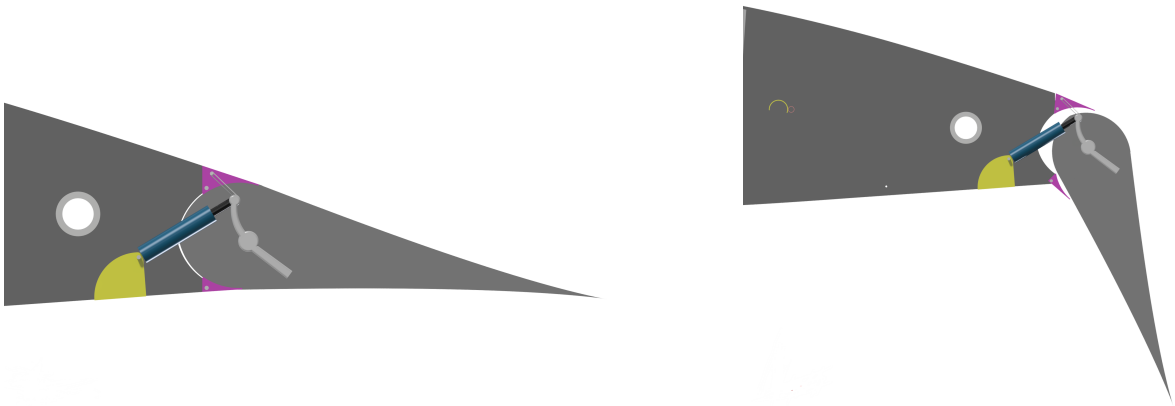

Figure 4.11: *Karfi*'s Wing Control Surfaces

The flaperons have the capability to be lowered to an angle of 80° which results in a large reduction in hover download. Flaperons also create a significant increase in lift when deployed which lowers the aircraft stall speed much more than a standard flap-aileron design. This allows the aircraft to transition into forward flight at lower airspeeds and creates a larger transition corridor for the tiltrotor.

5 Empennage Design

5.1 Vertical and Horizontal Tail Design

The horizontal and vertical tails, in conjunction with the elevator and rudder, provide stability and control for the aircraft in pitch and yaw during forward flight. *Karfi* has the added complication of having to accommodate two rear mounted turbofan engines as well as an aft-loading cargo door. With these goals in mind, *Karfi* employs a Π-tail design. The Π-tail allows the turbofans to be placed on the empennage within the tail structure, thus eliminating the need for engines mounted outside the fuselage where they would add considerable drag due to the increase in frontal area. A V-tail configuration was also considered, however, due to the complex mixing of pitch and yaw controls and historical stability issues with V-tail aircraft, such a design was not chosen. The V-tail would also require additional structural rigidity and support which would add to the empty weight of the aircraft.

The vertical tails were spaced in order to accommodate the turbofan engines in between them. They were extended vertically in order to ensure enough clean airflow over the tail and rudder to provide adequate yaw stability and control. To minimize the risks of local shocks occurring between the engine cowling and flow separation occurring over the vertical tail due to the complex interactions with the engines, *Karfi* has integrated the leading edge of the outboard cowling profile into the vertical tail. The trailing edges include a patch surface which adds volume to the body and reduces the flow diffusion.

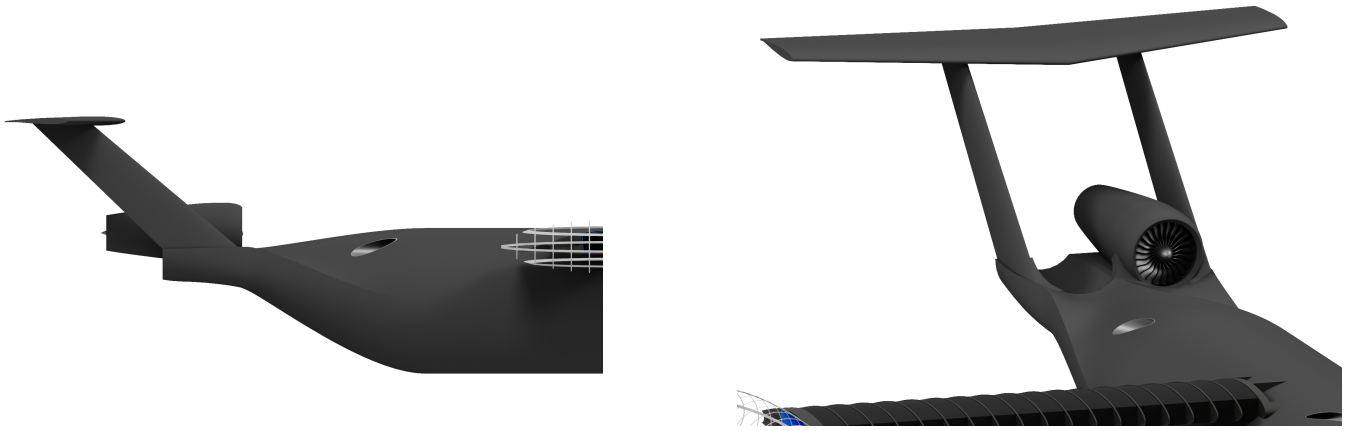

Figure 5.1: Empennage Design

The size of the empennage was calculated using horizontal and vertical tail volume coefficients based on historical data for similar size and structure aircraft to *Karfi*. A horizontal tail volume coefficient of 0.9 and a vertical tail volume coefficient of 0.08 were chosen. The sweep and taper were based on historical data for high speed aircraft.

The vertical tail has a symmetric airfoil of 15% thickness-to-chord ratio to allow for sufficient stiffening of the horizontal tail under dynamic loading. Due to the center of gravity being located close to the center of lift of the wing, the horizontal tail also employs a symmetric airfoil to avoid pitching the aircraft in level flight. The elevator and rudder provide the necessary lift to control and stabilize the aircraft in other flight conditions. The airfoils selected for the vertical and horizontal tail were NACA 0015 and NACA 0009, respectively. A summary of the empennage parameters is shown in the Table 5.1.

Surface	**Horizontal Tail**	**Vertical Tail (each)**	**Elevator**	**Rudder**
Area [**ft**^{2}] (m^2)	**168.3** (15.64)	**44.9** (4.17)	**48.8** (4.53)	**23.3** (2.17)
Span [**ft**] (m)	**27.23** (8.3)	**8.21** (2.5) (clearance)	**23.9** (7.28)	**7.9** (2.41)
Mean Chord [**ft**] (m)	**6.18** (1.88)	**5.47** (1.67)	**2.04** (0.62)	**2.95** (0.9)
Aspect Ratio	**4.4**	**1.5**	**11.7**	**2.7**
Sweep (degrees)	**5**	**50**	**N/A**	**N/A**
Taper Ratio	**0.6**	**0.75**	**1:1**	**1:1**

Table 5.1: Summary of Empennage Parameters

5.2 Turbofan Placement

With the goal of minimizing the additional frontal area added to the aircraft, the turbofan engines were partially embedded into the fuselage. The empennage surface slopes downward with two separate cuts to accommodate the engines. The turbofans directly ingest about 40% of the flow boundary layer over the fuselage which results in a propulsive efficiency benefit between 2-4%. The engine cowlings are joined by a patch surface to prevent local shocks in the area between the lower half of the engine structure which would cause an increase in drag [22].

6 Vehicle Performance

2emTable 6.1 summarizes the segment by segment vehicle performance over the course of the entire mission profile described in 1.1.3.

	Mission Segment											
Parameter	**1**	**2**	**3**	**4**	**5**	**6**	**7**	**8**	**9**	**10**	**11**	**12**
Mode of Flight*	**H**	**H**	**TCA**	**TCA**	**A**	**TCA**	**H**	**TCA**	**TCA**	**A**	**TCA**	**H**
Airspeed **[kts]** (km/h)	-	-	**200** (370.4)	**450** (833.4)	**200** (370.4)	**450** (833.4)	-	**200** (370.4)	**450** (833.4)	**200** (370.4)	**450** (833.4)	-
Total Turboshaft Power Required **[hp]** (kW)	**776.7** (579.2)	**8,204** (6,118)	**4,435** (3,307)	**10,056** (7,499)	**652.3** (486.4)	**15,280** (11,394)	**6,890** (5,138)	**3,879** (2,893)	**9,268** (6,911)	**652.3** (486.4)	**14,180** (10,574)	**5,875** (4,380)
Total Turboshaft Power Available **[hp]** (kW)	**8,688** (6,479)	**8,688** (6,479)	**8,688** (6,479)	**5,324** (3,970)	**8,688** (6,479)	**8,688** (6,479)	**8,688** (6,479)	**8,688** (6,479)	**5,324** (3,970)	**8,688** (6,479)	**8,688** (6,479)	**8,688** (6,479)
Turboshaft SFC **[lb/hp-h]**	**0.682** (0.415)	**0.370** (0.225)	**0.367** (0.223)	**0.385** (0.234)	**0.697** (0.424)	**0.358** (0.218)	**0.370** (0.225)	**0.367** (0.223)	**0.385** (0.234)	**0.697** (0.424)	**0.358** (0.218)	**0.370** (0.225)
Turbofan Thrust Required **[lb]** (N)	-	-	**1,397** (6,215)	**5,461** (24,292)	-	**8,016** (35,657)	-		**5,461** (24,292)	-	**8,016** (35,657)	-
Turbofan Thrust Available **[lb]** (N)	-	-	**1,829** (8,138)	**8,526** (37,926)	-	**14,250** (63,387)	-		**8,526** (37,926)	-	**14,250** (63,387)	-
Turbofan TSFC **[lb/lb-h]** (kg/kN-h)	-	-	**0.51** (51.8)	**0.51** (51.8)	-	**0.51** (51.8)	-	**0.51** (51.8)	**0.51** (51.8)	-	**0.51** (51.8)	-
Specific Range **[nm/lb]** (km/kg)	-	-	-	**0.036** (0.145)	-	**0.022** (0.091)	-	-	**0.039** (0.158)	-	**0.024** (0.098)	-
Endurance **[hr]**	-	-	-	**2.71**	-	**1.61**	-	-	**2.78**	-	**1.72**	-

*Mode of Flight Definitions: (H) Helicopter Mode, (A) Airplane Mode, (TCA) Thrust-Compounded Airplane Mode

Table 6.1: Mission Performance Data

6.1 Aerodynamic Data

Karfi's mission profile is dominated primarily by the cruise segments, totaling 450 nm (833.4 km) out of the 500 nm (926 km) mission radius. Consequently, an accurate representation of the vehicle drag and lift is essential in order to properly evaluate the vehicle's performance.

The lift, drag and moment areas/volumes at zero degrees of vehicle pitch and yaw were determined in the following manner. Using analysis of solid bodies in the CAD model for the aircraft, the surface and frontal areas of the necessary components were determined. For drag area, the C_D breakdown by component for the XV-15, [23], was used in conjunction with the previously determined frontal areas, equation 4. The lift areas were by taking the surface areas of the wing and horizontal tail.

$$\frac{D}{q} = C_D S_{ref} \tag{4}$$

The component moment volume for the fuselage was found by taking the overall volume of the fuselage, while for the horizontal tail, the surface area was multiplied by the distance between the wing's quarter chord and that of the horizontal tail.

Component	Drag Area [**ft**^{2}] (m^2)	Lift Area [**ft**^{2}] (m^2)	Moment Volume [**ft**^{3}] (m^3)
Fuselage	**5.91** (0.55)	**-**	**2,989.0** (84.64)
Wing	**12.84** (1.19)	**548.1** (50.84)	-
Horizontal Tail	**2.11** (0.20)	**168.3** (15.64)	**6,651.2** (188.34)
Vertical Tail	**0.67** (0.06)	**-**	**-**
Nacelle	**0.78** (0.07)	**-**	**-**
Proprotor Hub	**0.62** (0.06)	**-**	**-**
Turbofan Engine	**0.91** (0.08)	**-**	**-**
Total	**23.83** (2.21)	**716.4** (66.48)	**9,640.2** (272.94)

Table 6.2: Lift and Drag Area Component Buildup

The parasitic side force area was also investigated in a similar manner to the drag area, by finding the side area of the aircraft with the use of the CAD model. It was found that it equaled 597.18 ft^2.

As mentioned in Section 3.3.3, optimizing figure of merit allows for significant improvements in efficiency for a high speed tiltrotor design. Figure 6.1 demonstrates that as blade loading is increased, figure of merit exponentially increases. A blade loading of 0.15 was picked due to the increase in figure of merit after this point becoming marginal. As a result, *Karfi* has a figure of merit of 0.85 at a gross takeoff weight of 46,829 lb (21,241.3 kg).

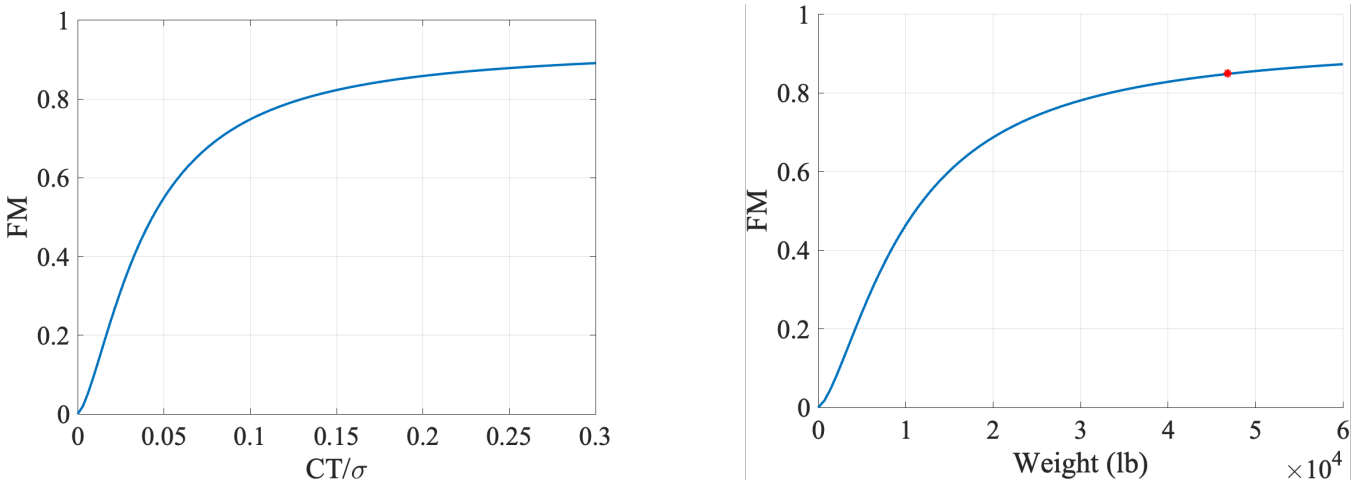

Figure 6.1: Figure of Merit versus C_t/σ and Weight

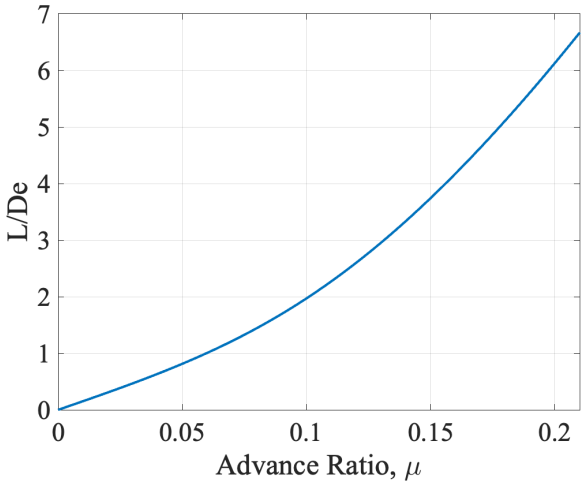

Figure 6.2: Rotor Lift to Drag Ratio as a Function of Rotor Advance Ratio in Edgewise Flight

Figure 6.2 shows the evolution of lift to drag ratio of the main proprotors as forward speed of the aircraft increases during edgewise flight. As the vehicle increases in speed, its performance also increases due to decreasing power required. This occurs because as advance ratio increases, air is being forced into the proprotors instead of being pulled in. Figure 6.2 also demonstrates a high L/D_e ratio which is due to the proprotors being designed optimally for high thrust conditions (hover).

6.2 Hover Performance

Per the RFP, the aircraft is required to hover at 2,000 ft (609.6 m) 85°F (29.44°C) atmospheric conditions, running at 90% of engine MRP. The download from the proprotors is 338.8 lbs (153.7 kg) which is equivalent to an additional 0.72% of the SDGW.

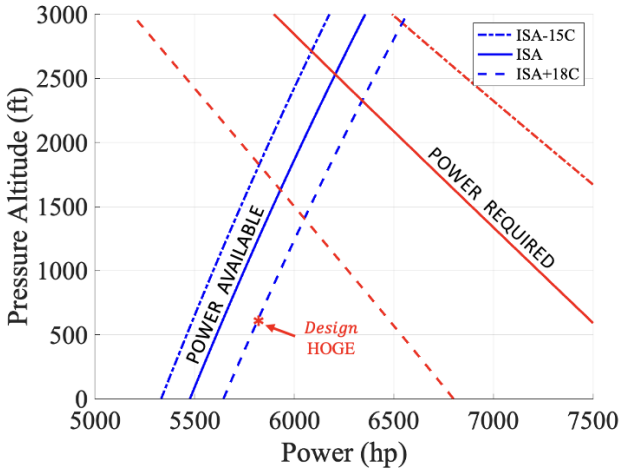

Figure 6.3: *Karfi* Hover Performance

Figure 6.3 illustrates the power required and power available for hover at GTOW against altitude at various atmospheric conditions. At the hover design point, the vehicle requires 7,800.7 hp (5,817 kW) to

hover, less than the power available of 8,683.1 hp (6,475 kW). Thus, at the hover design point, *Karfi* has approximately a 10% excess of power. Additionally, Figure 6.4 demonstrates the altitude at which the power required to hover at GTOW equals the power available from the engines, also known as the hover ceiling. In *Karfi*'s case, this point lies at 4,614.5 ft (1406.5 m) in altitude for ISA+59°F (15°C) conditions.

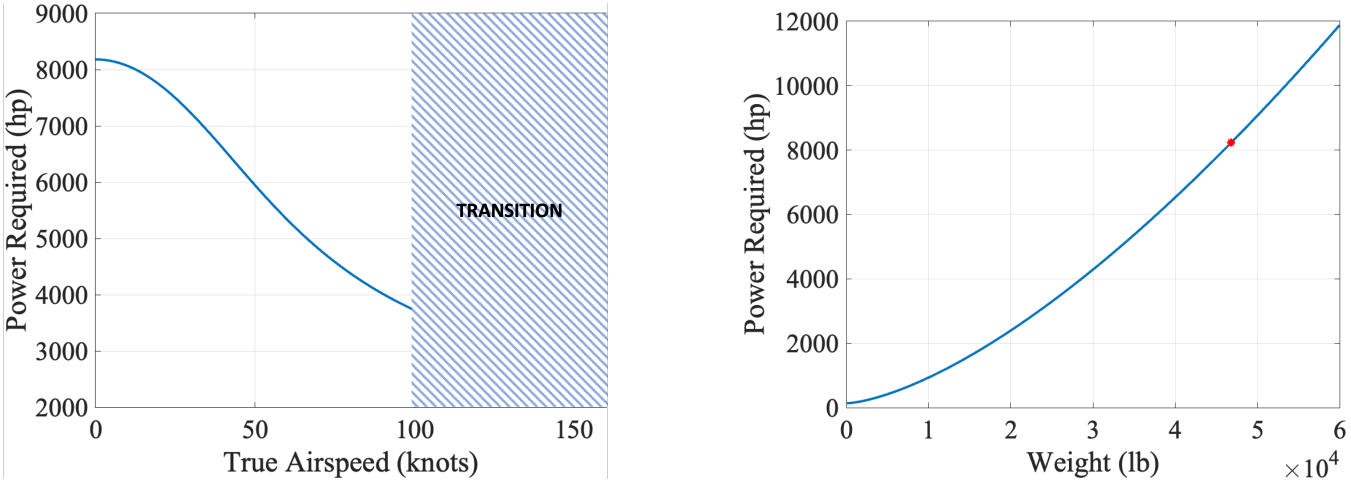

Figure 6.4: Figure of Merit versus Velocity and Weight

Figure 6.4 shows the power required at different velocities and vehicle weights in edgewise flight mode when the turbofans are idling. *Karfi* uses turbofan thrust to transition to forward flight once it reaches 48 kts (88.9 km/h).

6.3 Forward Flight Performance

The aircraft equipped solely with turboshaft engines is incapable of reaching the required cruise speed of 450 kts (833.4 km/h) for the mission profile. Initial analysis was conducted where the turboshaft engine provided power for both conditions, hover and forward flight; however, it was determined that this method lead to a significant gross takeoff weight, approximately 60,000 lb (27,215.5 kg). It was decided that for forward flight, it was necessary to supplement the turboshaft engine power with turbofan engines. Numerous combinations of turboshaft and turbofan engine power/thrust ratios were analysed. It was found that sizing the turboshaft engines solely for hover provided the lowest gross takeoff weight and fuel required for this mission. Thus, in the propeller mode, the proprotor supplies whatever thrust that is available from the turboshaft engines and the rest of the required thrust is supplied by the two turbofan engines, Figure 6.5.

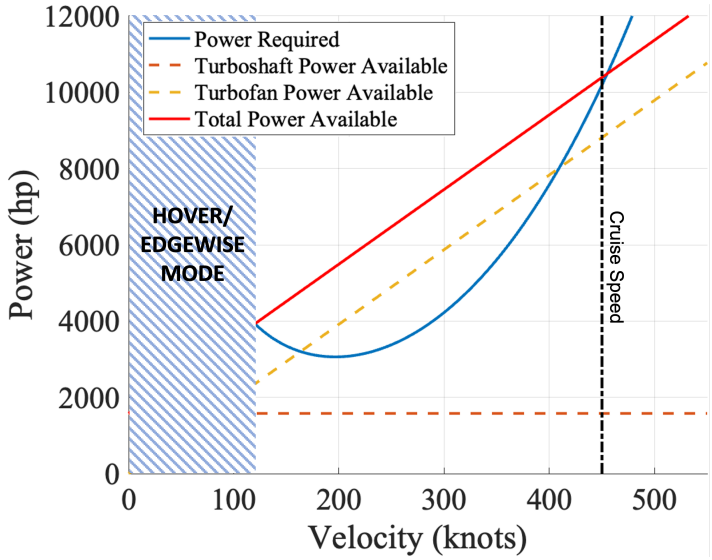

Figure 6.5: Total Power Required vs Airspeed from Hover to Maximum Continuous Power Speed

Figure 6.5 shows a breakdown of the power available and power required from hover to maximum continuous power. In forward flight, the turboshaft engines provide a constant power. The turbofan engines are then used to supplement the turboshaft engines in order to produce the necessary power required at any given speed condition. At maximum continuous power, *Karfi* is able to cruise at the desired 450 kts (833.4 km/h).

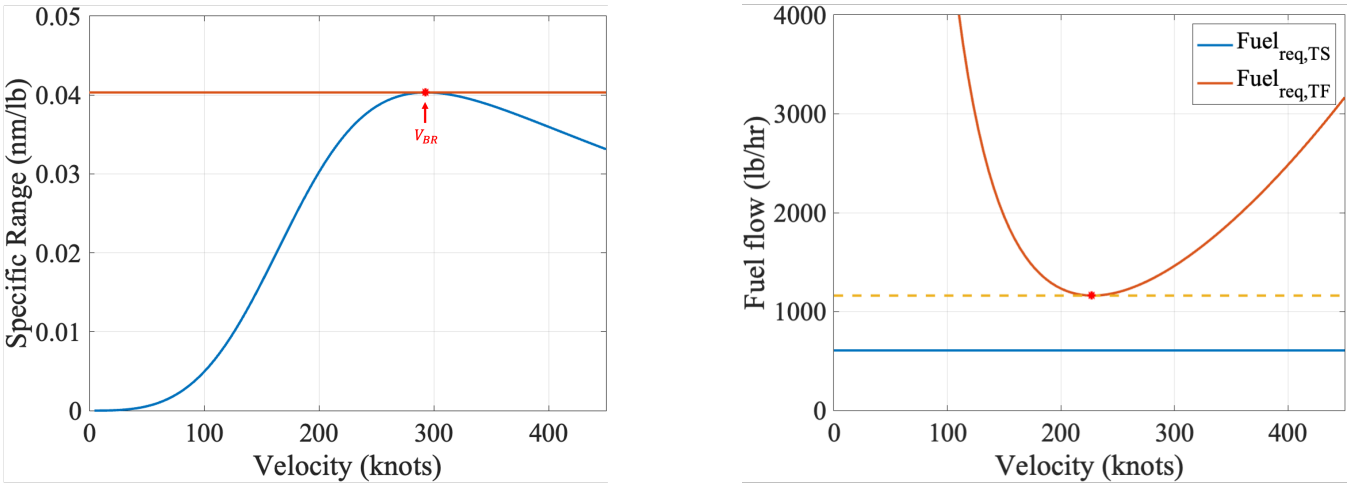

Figure 6.6: *Karfi*'s Specific Range (left) and Fuel Flow (right) vs Velocity

Figure 6.6 shows the specific range and fuel flow of *Karfi* as a function of forward velocity. The best range velocity was found to be $V_{BR} = 293$ kts (542.6 km/h) and the best endurance velocity was found to be $V_{BE} = 227.3$ kts (420.9 km/h).

6.4 Full Operational Envelope

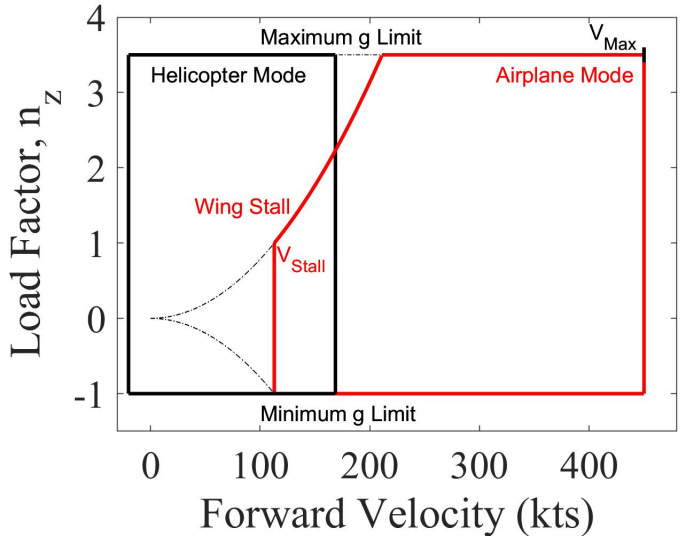

Figure 6.7: V-N$_z$ Diagram for *Karfi*

Two V-Nz diagrams are needed to define *Karfi*'s different flight modes. The flight envelopes represent the aircraft's structural capability in helicopter mode and airplane mode, respectively (Fig. 6.7). The envelope is bounded by stall limits, tip speed drag limits, and the RFP maneuvering limits. Helicopter mode was defined as when the proprotors are not tilted more than 45 degrees from the vertical. The helicopter mode envelope is simple, the aircraft is able to fly up to 168.64 kts (312.32 km/h), therefore the helicopter mode operations are bound only by the maneuvering limit loads. In forward flight mode, the aircraft still receives supplemental lift as the proprotors are aligned with the aircraft angle of incidence. However, this is much lower lift than is provided in helicopter mode and the flight envelope is still limited by the wing stall speed as well as the limit loads. V$_{stall}$ was calculated to be 112.9 kts (209.09 km/h).

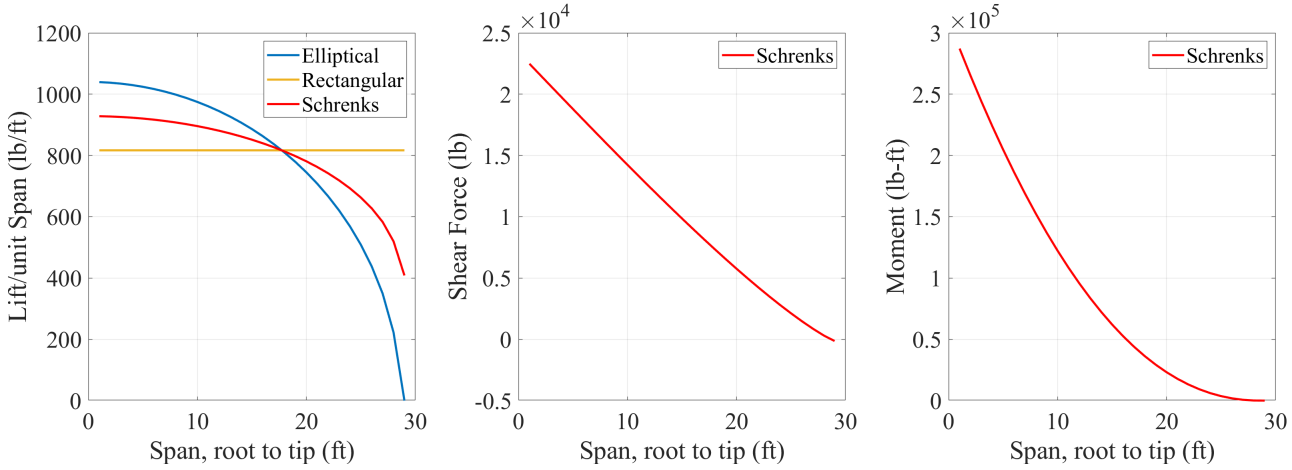

Figure 6.8: Wing Loads in 1 g Flight

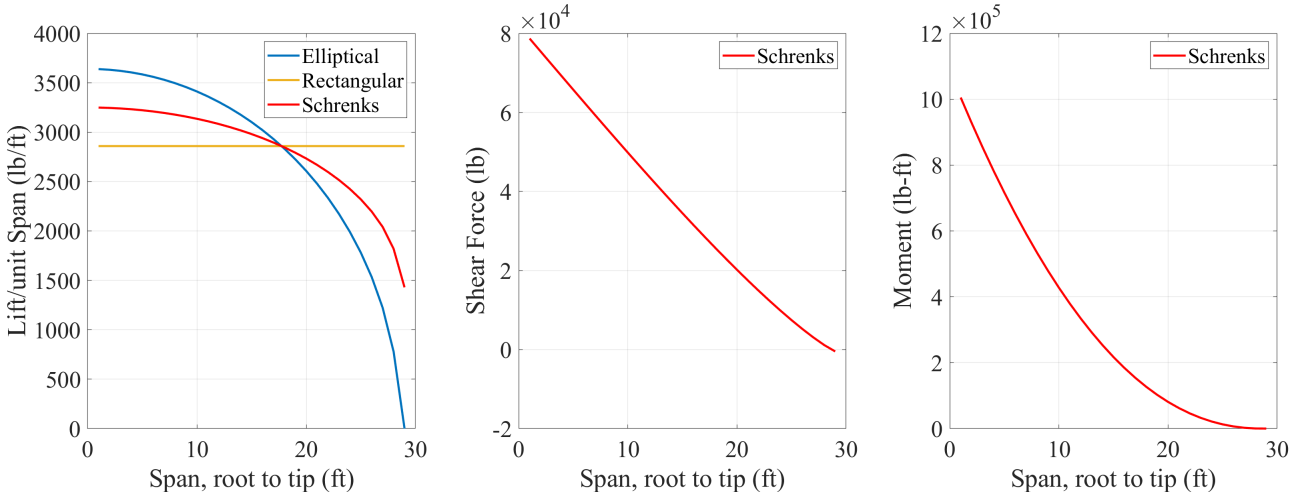

Figure 6.9: Wing Loads in 3.5 g Flight

Schrenck's Approximation was used to evaluate the loads acting on the aircraft, [24]. The lift per unit span distribution was first modeled as both an elliptical and rectangular distribution, the final approximation was calculated as the average of the two models. From this approximation, the lift, shear force, and bending moments were calculated for the length of the wing. Figures 6.8 and 6.9 show the loads on the wings of *Karfi* in 1 g and 3.5 g flight (limit load factor).

It was found that the maximum lift per unit span in straight and level flight is 928.1 lb/ft (1,381.2 kg/m) and is located at the root of the wing; while the minimum lift per unit span is 408.4 lb/ft (607.8 kg/m) and is located at the tip of the wing. When the design load factor is applied, the maximum lift per unit span is 3,248.39 lb/ft (4,834.1 kg/m), located at the root, while the minimum lift per unit span is 1429.46 lb/ft (2,127.3 kg/m). Under the design load factor, the maximum shear force and bending moments found for the wing are 78,677.8 lbs (35687.6 kgs) and 1,005,170 lb-ft (138,970 kg-m), respectively, both located at the root of the wing. the wing was designed such that the structure is able to handle both the shear force and bending moment seen with the design load factor applied while still maintaining an appropriate margin of safety. The design loads acting on the fuselage and empennage sections of the aircraft were not approximated with a model, as to evaluate the loads with any degree of certainty would require flight mechanics analysis which is not possible at this time.

7 Propulsion and Transmission Design

Based on the RFP requirements, *Karfi* is designed to be a high speed cargo VTOL aircraft. Because of this, the aircraft has an unconventional configuration. In order to achieve VTOL capabilities, it is a tiltrotor, with two proprotors at the wing-tips, each with a turboshaft engine to provide power. In order to fulfill the requirement of 450 kts (833.4 km/h) cruise speed at 20,000 ft (6,096 m), the proprotors are equipped with a two-speed transmission to keep the rotor tip speeds below the Mach divergence number of 0.85. Additionally, there is a pair of turbofan engines mounted near the tail to provide additional thrust for forward flight. Together, these engines can propel the aircraft to 450 kts (833.4 km/h) at 20,000 ft (6,096 m) while also maintaining VTOL capabilities.

7.1 Engine Selection

The aircraft requires an installed turboshaft power of 10,951 hp (8,054.5 kW) and an installed turbofan thrust of 14,420 lb (64,143.3 N).

7.1.1 Turboshaft Design

The turboshaft engines used to power *Karfi*'s proprotors were sized using the engine data provided in the 2007 VFS SDC RFP [16]. This model uses a 1,002 hp (747.19 kW) engine as a baseline and then uses a series of scaling equations to adapt the engine properties for a set of requirements.

Advanced Engine Data for SL/ISA Conditions

Engine Rating	Duration	Power Available (hp)	SFC (lb/hp.hr)
OEI	30 sec	1,049	0.360
MRP	2 min	1,002	0.361
IRP	30 min	934	0.365
MCP	continuous	764	0.379
Part Power	-	501	0.426
Idle	-	200	0.672

Figure 7.1: Engine Data Provided in VFS's 2007 RFP

The scaling was accomplished using the procedure in [16]. This method resulted in the turboshaft engines having the specifications listed in Table 7.1, as well as having a performance envelope as described in Table 7.2.

Specification	**Value**
Installed Power **[hp]** (kW)	**10,951** (8,054.45)
Max Continuous Power **[hp]** (kW)	**5,475.5** (4,027.22)
Specific Fuel Consumption | **[lb/lb-h]** (kg/kW/h)	**0.322** (0.196)
Weight **[lb]** (kg)	**1,055.59** (1,281.2)
Diameter **[in]** (m)	**19.71** (0.5)
Length **[in]** (m)	**41.98**

Table 7.1: *Karfi* Turboshaft Engine Specifications

Engine Rating	Actual Power **[hp]** (kg/kW/h)	Actual SFC **[lb/hp-h]** (kg/kW-h)
OEI	**5,732.3** (4,216.1)	**0.306** (0.186)
MRP	**5,475.5** (4083.1)	**0.306** (0.186)
IRP	**5,103.9** (3,753.9)	**0.310** (0.188)
MCP	**4,174.9** (3,070.6)	**0.322** (0.196)
Part Power	**2,737.75** (2,013.6)	**0.362** (0.220)
Idle	**1,092.9** (803.83)	**0.570** (0.347)

Table 7.2: Turboshaft Engine Data

7.1.2 Turbofan Design

First, the thrust required was calculated from Equation 5.

$$\frac{F_{max}}{F_0} = 0.93 * \theta * (1 - 0.73M + 0.53M^2) \tag{5}$$

The density ratio (θ) at the given flight condition is 0.533, the Mach number (M) is 0.78, and F_0 is 14,420 lb (64,143.3 N) [5]. This equation provides the max thrust required for cruise, F_{max} = 4,087.5 lb (18,182.1 N).

Next, a bypass ratio was chosen using Torenbeek's model [5], which gives a relationship between thrust specific fuel consumption and bypass ratio for specific operating conditions settings.

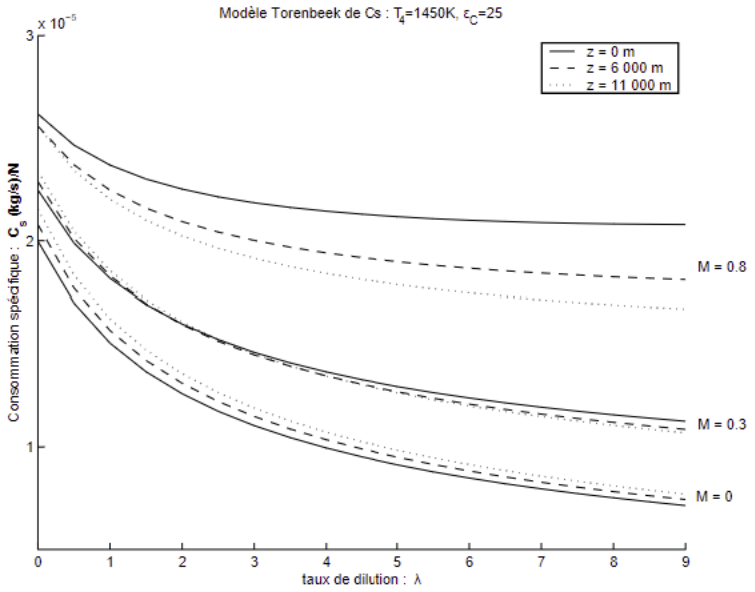

Figure 7.2: Torenbeek Model: TSFC vs Bypass Ratio for Turbofans at Specific Operating conditions [5]

According to Figure 7.2, at 19,685 feet (6,000 m) in altitude and a Mach of 0.8, significant gains in fuel efficiency occur until a bypass ratio of 4 is reached. Afterwards, diminishing returns occur when taking into account that frontal area increases steadily with increasing bypass ratio, leading to increases in drag. As a result, a bypass ratio of 4 was chosen.

Although the Torenbeek model provides a corresponding thrust specific fuel consumption for the chosen bypass ratio, the LEAP-1C engine specifications were used to design *Karfi*'s rubberized turbofan engines since it is the most modern turbofan engine with a thrust specific fuel consumption of 0.51 [25]. Equations 6 and 7 were used to calculate the weight of the turbofan engines where F_0 is in Newtons, mass of dry engine (M_{dry}) is in kg and the installation factor $k_{install}$ is 1.2.

$$M_{dry} = 22.2 * 10^{-3} F_0 \tag{6}$$

$$M_{engine} = k_{install} M_{dry} \tag{7}$$

The turbofan total engine wet weight was found to be 3,118 lb (1,414.301 kg).

Finally, given data from existing turbofan engines, models were built to create working equations to calculate the length and diameter of the turbofans based on installed thrust, Figure 7.3.

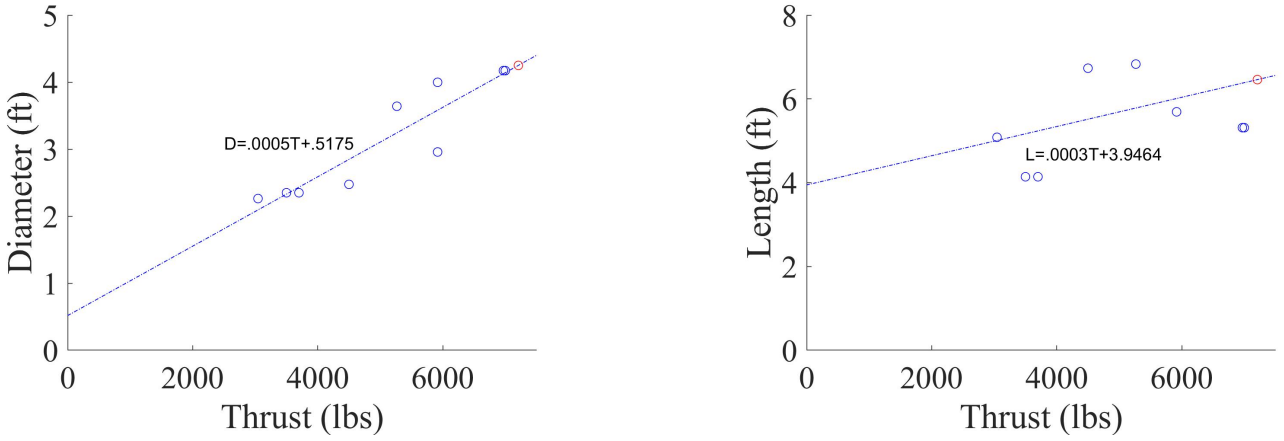

Figure 7.3: Turbofan Engine Sizing

Using these models, the size of turbofans (represented by the red circle on the above figures) were found and Table 7.3 summarizes the results of this section.

Parameter	**Engine (Each)**	**Engine (Both)**
Installed Thrust **[lb]** (N)	**7,210** (32,071.7)	**14,420** (64,143.4)
Dry Weight **[lb]** (kg)	**1,559** (707.15)	**3,118** (1,414.3)
Wet Weight **[lb]** (kg)	**1,871** (848.67)	**3,742** (1,697.3)
TSFC **[lb/lb-h]** (kg/kN-h)	**0.51** (51.8)	-
Length **[ft]** (m)	**6.46** (1.98)	-
Diameter **ft** (m)	**4.25** (1.30)	-

Table 7.3: *Karfi* Turbofan Specifications

7.2 Transmission Design

The turboshaft engines can be assumed to have a factory-made gearbox that takes the 18000 RPM power turbine and converts it to 6,000 RPM. The power generated by the engines must be transmitted to the proprotors and stepped down from 6,000 RPM to 346 RPM in hover.

7.2.1 Drive System

In order to go from 6000 rpm to 346 rpm, the transmission requires a 17.34 reduction ratio. Since the engines are located in the fuselage, a drive shaft is needed through the wing in order to power the proprotors. Having the reduction take place as close to the rotor as possible reduces the size and weight of the driveshaft that must span the full length of the wing. If all the reduction is done in the fuselage, the drive shaft would weigh 513 lb (232.69 kg). With most of the reduction done in the nacelle the driveshaft weight is reduced to 63 lb (28.6 kg). With the engine mounted in the fuselage, the weight of the gearbox primarily being in the nacelle is not a problem.

Drive System Section Component	**Bevel 1** Pinion : Gear	**Spur** Pinion : Gear	**Bevel 2** Pinion : Gear
Teeth	23 : 15	49 : 16	93 : 38
Gear Ratio	1.53	3.06	2.45
RPM	6,000 : 3,913	3,913 : 1,278	1,278 : 522.1

Table 7.4: Drive System Gear Design Summary

7.2.2 Two-Speed Clutching System

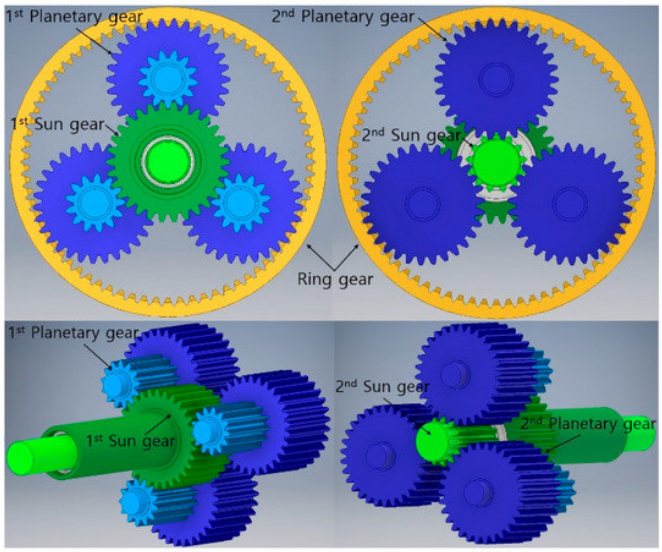

Figure 7.4: Two-Speed Clutch [6]

The drive shaft enters the 2-speed clutching system with an RPM of 522.08. The planetary gear clutch system enforces a 1.51:1 reduction ratio when disengaged which provides the *Karfi*'s VTOL mode RPM of 345.8. When engaged the planetary gear system has a reduction ratio of 3.08:1 which gives a forward flight mode RPM of 169.5. The gears were sized such that the planetary gears for the engaged and disengaged states rotate on the same axis. The clutch-engaged planetary gears will always be in contact with the ring gear, but will not always be driven directly. When the clutch is not engaged the larger disengaged sun gear drives the planet gear system through contact with the smaller disengaged gears, the larger gears in turn drive the ring gear. When the clutch is engaged the large planet gears are driven by the smaller sun gear and drive the ring gear with a larger gear ratio for a more substantial rpm reduction.

Clutch Status Component	**Engaged** Sun : Ring	**Disengaged 2** Sun : Ring
Teeth	25 : 77	51 : 77
Gear Ratio	3.08	1.51
RPM	522.1 : 169.5	522.1 : 345.8

Table 7.5: Planetary Gear Clutch System Gear Design Summary

8 Airframe Structural Design

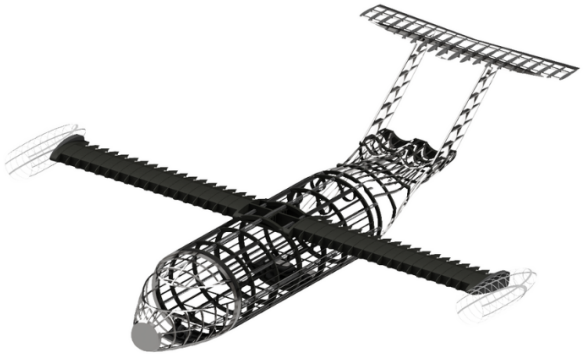

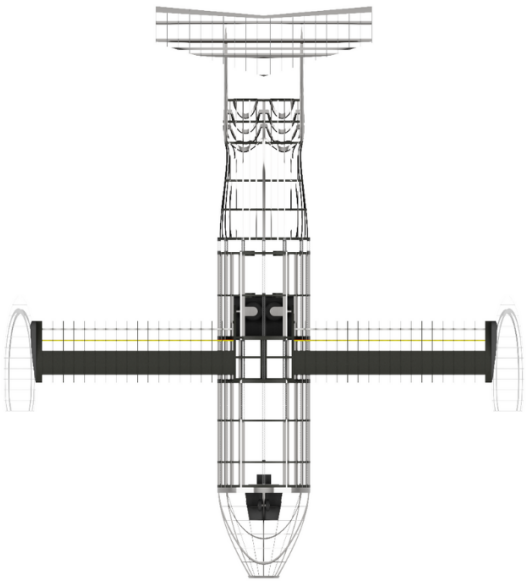

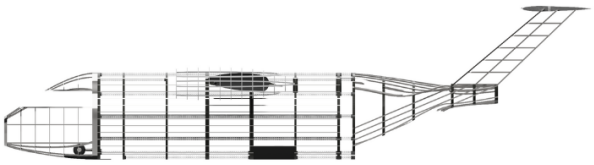

UNIVERSITY OF MARYLAND

KARFI

8.1 Airframe Structure

In the fuselage structure, wound composite structures similar to isotruss have been implemented to replace conventional longerons within the fuselage structure. These structures possess exceptional strength-to-weight ratios and demonstrate robust fatigue resistance, enabling them to effectively distribute loads and manage stress levels.

As a result of this design choice, the fuselage weight has been reduced by approximately 15% compared to a traditional structure. This substantial weight reduction not only enhances the overall performance of the aircraft but also contributes to improved fuel efficiency and increased payload capacity. Moreover, this accomplishment parallels the outcomes observed in the 'Gamera – The Human Powered Helicopter' project, wherein the utilization of analogous wound composite structures resulted in a significant 20% decrease in empty weight [18].

8.2 Fuselage

Figure 8.1: Fuselage Layout

8.2.1 Turboshaft Integration

The aircraft design incorporates a seamless integration of turboshaft engines into the fuselage, positioned behind the wing. This specific placement was carefully selected to optimize the aircraft's performance and prioritize safety considerations.

Throughout the design process, various alternative configurations were explored, including partially embedded turboshaft engines and wingtip nacelle embedding. However, these options were deemed less favorable due to increased drag area and/or additional structural load implications on the wing. The deci-

sion to embed the engines within the fuselage resulted in a more aerodynamically beneficial configuration, leading to improvements in speed and fuel efficiency. Placing the engines within the fuselage instead of the nacelle allows for an increase in bending frequency (due to a decrease in weight at the wing tips), leading to a higher whirl flutter onset velocity.

The integration of the engines into the fuselage structure, complemented by the implementation of advanced thermal insulation materials like ceramic fiber insulation, serves a dual purpose. It effectively mitigates noise and infrared signature emissions while providing an additional layer of protection against potential hazards, such as bird strikes or debris. By minimizing the risk of engine failure causing damage to critical components, this design approach ensures both operational reliability and passenger safety.

Thermal management concerns were addressed through the meticulous design of an angled exhaust shaft. This solution directs the expulsion of hot exhaust gasses away from the aircraft body as well as the intakes of the rear turbofan engines. Consequently, it safeguards the aircraft from potential thermal damage and sustains the long-term efficiency and reliability of the turbofan engines.

Another noteworthy design aspect involves the utilization of a divergent nozzle as the intake for the turboshaft engines. The nozzle is engineered with a specific cross-sectional area ratio (A_2/A_1) of 3.6, optimizing the intake airflow, modifying M = 0.72 at the intake entrance, to M = 0.2 at the front of the turboshafts. This optimization results in improved overall aircraft performance and reduced fuel consumption.In addition, appropriately located access panels in the fuselage will provide easy access to the engine for routine maintenance.

To summarize, the integrated turboshaft engine configuration offers significant benefits, including reduced drag, enhanced fuel efficiency, minimized noise and infrared signatures, improved protection against hazards, optimized airflow management, and effective thermal insulation. These design choices were made with a strong focus on enhancing aircraft performance and ensuring safety.

In order to operate from unprepared zones, an Auxiliary Power Unit (APU) system is necessary when surrounding infrastructure is lacking, such as no surrounding ground power.The exhaust of the APU is shared with that of the turboshaft embedded in the fuselage.

Infrared Supressor

The Infrared (IR) suppressor reduces the temperature of the turboshaft engine exhaust gases and enhances the survivability of *Karfi*, by reducing its heat signature. Located at the exhaust outlets of turboshaft engines, the suppressor is a part of the exhaust system itself, encasing the exhaust outlet and extending the path that the gases must travel before being expelled. This extended path, lined with heat-resistant material, allows more time for the gases to cool down and for the cool ambient air to be introduced and mixed with the hot gases. The design maximizes the cooling effect while minimizing any potential negative impact on engine performance. A turboshaft engine with an infrared suppressor only loses approximately 2.5% power during hover in-ground effect (HIGE), [26].

This integrated feature enhances the low observability characteristics of the aircraft, playing a critical role in hostile environments where heat-seeking threats are prevalent. It is an essential component of *Karfi*'s comprehensive approach to maximizing the survivability of the mission.

8.2.2 Pressurization

The RFP requires a minimum cruise altitude of 20,000 ft (6,096 m), thus the cabin will need to be pressurized for crew safety and comfortability. The international standard for aircraft is to be pressurized to an equivalent altitude of 8,000 ft. Based on the difference in air density at 8,000 ft (2,438.4 m) and

20,000 ft (6,096 m) altitude and the volume of the cabin, the pressurized air would result in 35.8 extra pounds (16.2 kgs) (111.1 total lbs of pressurized air) (50.4 kgs) being carried by the aircraft. The cabin will be pressurized through a bleed-air system. A standard airplane cabin replaces all of its air about every 3 minutes. Assuming that is done at a constant rate, the bleed-air system will need to draw about 37 lbs (16.8 kgs) of air per minute in order to keep the cabin pressurized. Based on the information given about the Williams FJ44-2C in [27], and scaling to the size of our engine, pressurizing the cabin will result in a 0.82% loss of turbofan thrust in cruise.

8.3 Cargo Bay Door

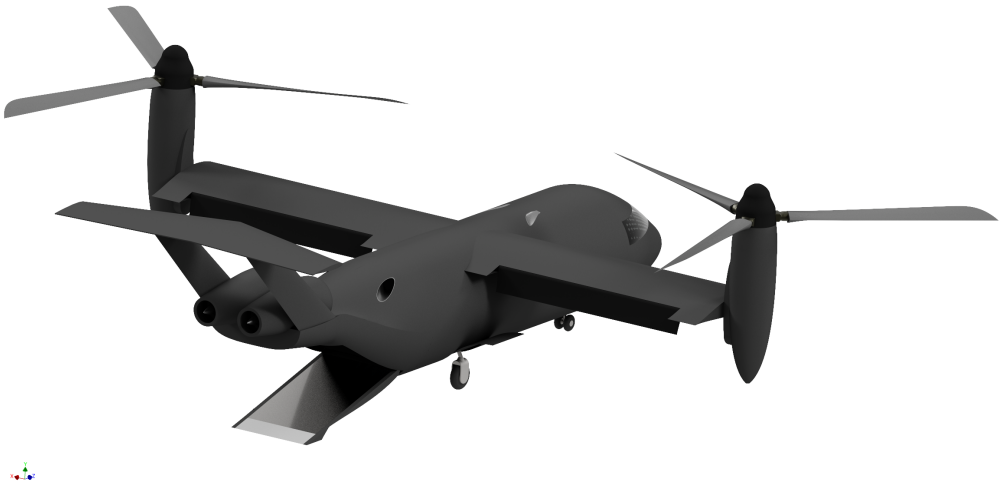

Figure 8.2: Cargo Bay Door

To achieve a more aerodynamically efficient fuselage, the rear fuselage is designed in a cone shape with the bottom angled upward. The door is made up of a single 13.5 ft (4.11 m) by 8.5 ft (2.59 m) rectangle, with the outer skin of the door shaped to fit on the rear of the fuselage. Two hydraulic jacks are utilized to actuate the movement of the cargo door, with one of their ends attached to the cabin wall. Due to the curvature of the outer skin of the door, the ramp portion of the door does not make contact with the ground on its own. A ramp extension is attached to the cargo bay door and extends out until it reaches the ground. This ramp provides a smooth transition between the ground and the cargo bay, facilitating easier loading or unloading of vehicles and equipment.

8.4 Landing Gear

The landing gear is designed to meet the RFP requirement of a 10 ft/s (3.048 m/s) sink speed landing. The landing gear was designed for both VTOL and (short takeoff and landing) STOL capabilities, however *Karfi* can only land when in helicopter mode. In order to land in airplane mode the landing gear would need to provide a ground clearance of over 9 ft (2.74 m) from the bottom of the fuselage which would cause lateral instability. Due to the high speed capabilities for which it was designed, *Karfi*'s landing gear needs to be retractable in flight to reduce drag. A tricycle landing gear configuration was chosen with these goals in mind.

Each landing gear has an oleo-pneumatic shock absorbing strut. The main landing gear struts have a

diameter of 4.735 in (.120 m), the nose gear strut has a diameter of 3.492 in (0.120 m). The struts have a length of 9.75 in (0.248 m) in order to meet the landing speed requirements. The main landing gears each have a single 30 (0.762) by 8.8 (0.224) in (m) tire. This was chosen in order to enable the landing gear to retract into the fuselage without the necessity for a sponson. The nose gear employs two 18 (0.457) by 5.5 (0.14) in (m) tires. The main gear and nose gear tires weigh 57 lb (25.86 kg) (each) and 14 lb (6.35 kg) (each) respectively [28].

The landing gear retracts into a compartment within the fuselage through the use of a hydraulic system to maintain smooth airflow. The landing gear is located such that the main gear is 15° aft of the aftmost center of gravity location to prevent rearward longitudinal tip-over. The main gears are placed over 18° laterally of the center of gravity on each side to provide lateral stability as well.

9 Avionics and Mission Equipment Package

Karfi is a military cargo aircraft meant for use in highly-contested environments. As a result, the environment in which it operates offers a variety of challenges and potential risks. The avionics bay and Mission Equipment Package (MEP) were designed to take into account *Karfi*'s environment of operation to best equip the pilots with the necessary technologies to safely and successfully complete the mission.

9.1 Avionics

9.1.1 Navigation

Global Positioning System (GPS)

Karfi incorporates a satellite-based GPS navigation system that delivers accurate position, velocity, and time data, ensuring safe and efficient navigation for pilots. Housed in the avionics bay, the GPS receiver processes signals from multiple satellites, with an exterior-mounted antenna on the fuselage top ensuring optimal reception. This precise real-time positioning would enable the pilots to navigate challenging environments such as mountainous terrain or low-visibility conditions. Furthermore, the GPS system supports instrument approach procedures, allowing for safe navigation even in instances of severely reduced visibility [29].

Automatic Flight Control System (AFCS)

During the design of the vehicle, the incorporation of a state-of-the-art Automatic Flight Control System (AFCS) to enhance flight efficiency, safety, and reduce pilot workload was made. The central component, the Flight Control Computer, resides in the avionics bay, where it processes real-time data from an array of onboard sensors. The AFCS also comprises servo actuators positioned near the control surfaces in the wings and tail, translating computer commands into physical control surface movements. We designed a user-friendly control panel within the cockpit, serving as the interactive interface for setting flight parameters and controlling various autopilot modes. This comprehensive AFCS is fundamental to our rotorcraft's operation, ensuring a perfect blend of automation and control for optimal performance.

Inertial Navigation System (INS)

Karfi's design features an autonomous Inertial Navigation System (INS) that calculates an aircraft's position, velocity, and orientation without relying on external signals. Installed in the avionics bay, the INS serves as a dependable backup navigation system, particularly when external signals are compromised or unavailable due to interference from natural or human-made sources. The INS comprises an Inertial

Measurement Unit (IMU), which contains accelerometers and gyroscopes, and a navigation computer that processes the sensor data. This autonomous operation ensures high update rates and immunity to external interference. The INS' ability to rapidly process and respond to changes in an aircraft's motion and orientation makes it ideal for supporting dynamic maneuvers, including complex, fast, or sudden changes in movement or flight path.

9.1.2 Communication

Very High Frequency (VHF) radio system

The design includes a Very High Frequency (VHF) radio system which ensures reliable communication with air traffic control (ATC) and other aircraft during flight. Comprising a VHF radio transceiver, located in the avionics bay, and an exterior-mounted antenna on the bottom of the fuselage, the system enables clear transmission and reception of voice and data communication over the frequency range from 30 to 300 MHz.

Ultra High Frequency (UHF) radio system

Karfi also houses Ultra High Frequency (UHF) radios as an additional communication tool. Similar to the VHF system, the UHF antenna is also mounted on the bottom of the fuselage. Although both UHF and VHF radio systems facilitate communication with air traffic control and other aircraft, they operate on distinct frequency bands. Specifically, UHF operates within the frequency range of 300 MHz to 3 GHz, while VHF operates within the 30 to 300 MHz range (Thomas). This difference in frequency range imparts unique characteristics to each system: UHF, with its shorter wavelength, is well-suited for penetrating obstacles, making it an excellent choice for transmissions through concrete buildings in the urban area [**?**].

Satellite Communication (SATCOM)

The Satellite Communication (SATCOM) system is integrated into the system for long-range, over-the-horizon communication capabilities, enabling global connectivity and facilitating communication with other command centers. The SATCOM antenna, mounted on the top or sides of the fuselage, allows for two-way data and voice transmission with communication satellites. Notably, the SATCOM system differs from the GPS system in its function: while GPS antennas receive signals from GPS satellites to determine precise location, altitude, and time, SATCOM antennas are designed to provide voice and data transmission capabilities beyond the horizon(Stephens and Whittington).

9.2 Mission Equipment Package

Besides reducing radar cross sectional area and infrared signature, threat avoidance takes the form of countermeasures in the case of detection. The Mission Equipment Package (MEP) was designed to give *Karfi* the highest possible survival rate by including counter measures to common threats.

9.2.1 Countermeasures dispenser system (CMDS)

Dispenser units, mounted on the aircraft's exterior on the fuselage and tail, play a crucial role in deploying countermeasures to protect the aircraft from threats. One such countermeasure is chaff, composed of small aluminum strips or metalized glass fibers. Another countermeasure is flares, which mimic the aircraft's high-temperature exhaust to attract heat-seeking missiles.

9.2.2 Directed Infrared Countermeasure (DIRCM) System

Directed Infrared Countermeasures (DIRCM) are advanced systems designed to safeguard the aircraft from infrared-guided surface-to-air or air-to-air missiles. These systems function by detecting incoming missile threats via an array of sensors constituting the Missile Warning System (MWS), distributed on the aircraft's exterior to achieve comprehensive 360° coverage.

The centerpiece of the Directed Infrared Countermeasures (DIRCM) system is a high-intensity, modulated laser. This laser is housed within a turret and mounted on the tail of the aircraft to ensure an unobstructed line of sight, critical for its operation. The role of this laser is to accurately target and confuse the infrared seeker head of an incoming missile, thereby causing it to deviate from its course.

The precision targeting of the laser is maintained by the Pointer-Tracker System. This system uses real-time data from the Missile Warning System (MWS), which continuously monitors the surroundings for missile threats. The Pointer-Tracker System takes this data and uses it to track the flight path of the detected missile, steering the laser to keep it focused on the missile's infrared seeker head.

The coordination of these components is managed by the Control Interface. Located within the avionics bay of the aircraft, the Control Interface processes the missile threat data from the MWS. Based on this information, it controls the operations of both the DIRCM and the Pointer-Tracker System, ensuring that these systems work together seamlessly to neutralize incoming threats.

9.2.3 Terrain-Following System

The Terrain-following system in our design allows aircraft to fly at very low altitudes, maintaining a constant height above ground level to evade enemy radar detection or safely navigate mountainous regions during missions. The system uses a Terrain-following Radar (TFR) to scan the terrain ahead by transmitting a pencil beam radar signal and calculating a real-time terrain profile based on the signal's travel time.

To guide the aircraft, the TFR system continuously computes a path that adjusts to the terrain while maintaining a pilot-selected clearance distance. This process involves comparing the actual angle to the terrain with a desired angle, generating an angle error, and adjusting the aircraft's altitude accordingly. Additionally, a radar altimeter, with its receiver housed in the avionics bay and an antenna mounted on the bottom of the fuselage, provides accurate altitude data relative to the ground, ensuring a safe altitude is maintained throughout the flight.

9.2.4 Search and Rescue Equipment

While *Karfi*'s primary use is to be a high-speed cargo and personnel transport vehicle, the aircraft can be utilized for other missions. With a disk loading of 19.5 lb/ft2, the aircraft can be utilized for search and rescue missions on a variety of unprepared surfaces. The only conditions that the *Karfi* would not be suitable for is dry sand or water spray which requires a disk loading of below 4.5 lb/ft^2 (47.88 Pa) for safe operations. With that said, our disk loading is within the Water rescue limit, allowing *Karfi* to safely operate as a water rescue aircraft.

To accommodate a rescue mission of this nature, a winch and cable system can be mounted to the rear of the aircraft at the cargo bay door opening. Locating the winch by the cargo bay doors allows for the furthest distance from the proprotors, minimizing the influence of the downwash/outwash on the operation of the winch and basket. A stokes basket, attached to the winch can be lowered from the rear of the aircraft to the surface of the water below, in which the rescue victim can be placed and lifted up to

the aircraft. Assuming that a rescue victim would weigh 250 lb (113.34 kg), *Karfi* would be able to rescue 20 victims at a time.

10 Vehicle Cost

To compute the cost necessary to build and maintain *Karfi*, NASA's Design and Analysis of Rotorcraft (NDARC) was used [14].

Component	**Cost ($)**
Wing	9,156,721
Rotor Systems	1,727,327
Fuselage	113,519,630
Turboshaft Engines	5,820,000
Turbofan Engines	6,500,000
Drive System	374,535
Avionics	993,279
Empennage, Nacelle and Landing Gear	2,250,255
Auxiliary Power System, Fuel and Propulsion Systems	25,781
Environmental Group	493,000
Armament, Furnishings, Loading and Handling	13,623,330
Aircraft Manufacturing Cost	154,483,858
Maintenance Cost per Hour	3,456

Table 10.1: *Karfi* Cost Analysis Results

11 Weight Breakdown

The weight analysis for *Karfi* was meticulously conducted, using the weight models from the U.S. Army Aero Flight Dynamics Directorate (AFDD) and NASA's Design and Analysis of Rotorcraft (NDARC), [13] [14]. The AFDD model provides a series of equations devised specifically for estimating distinct weight groups.

The total mission weight is calculated as the sum of the empty weight, crew weight, and payload weight. Simultaneously, the weight analysis also addressed the determination of the center of gravity (CG). The CG's longitudinal location was measured from the nose of the aircraft, while the vertical CG was referenced from the ground. The careful identification of these CG positions is crucial to ensure *Karfi*'s stability and control during flight.

Component	Weight (lb)	Weight (kg)
Wing Group	**2,634.15**	1,1194.9
Rotor Group	**2,790.82**	1,265.97
Proprotors (Total)	**1,443.31**	654.69
Rotor Hub	**1,111.18**	504.03
Spinner	**236.44**	107.25
Empennage Group	**1,066.66**	483.85
Horizontal Tail	**533.35**	241.93
Vertical Tail	**533.35**	241.93
Fuselage Group	**6,981.95**	3,167.13
Primary Structure	**6,099.07**	2,766.54
Pressurization	**487.93**	221.32
Crashworthiness	**395.22**	179.27
Landing Gear Group	**1,500.24**	680.53
Engine Gear Group	**5,649.15**	2,562.41
Turboshaft Engines (Total)	**2,111.18**	957.62
Turbofan Engines (Total)	**3,248.58**	1,473.56
Fluids	**289.39**	131.27
Air Induction Group	**1,086.71**	492.95
Nacelles (Total)	**974.41**	442.01
Air Induction	**112.29**	50.94
Fuel System Group	**582.62**	264.28
Drive System Group	**2,534.66**	1,149.70
Gearboxes (Total)	**1,712.34**	776.72
Rotor Shafts (Total)	**255.87**	116.06
Drive Shafts (Total)	**153.37**	69.57
Two-Speed Gearboxes (Total)	**342.47**	155.34
Flight Control Group	**1,417.05**	642.80
Hydraulic Group	**261.52**	118.63
Anti-Icing Group	**421.17**	191.05
Common Equipment Group	**1,458.60**	616.28
Avionics	**458.6**	208.017
Mission Equipment Package	**1,000**	453.59
Miscellaneous	**988.67**	448.45
Empty Weight	**29,373.95**	13,323.80
Crew (Total)	**750**	340.20
Payload	**5,000**	2,267.96
Fuel	**10,234.93**	4,642.56
Gross Weight (w/o 5% Margin of Empty Weight)	**45,358.88**	20,574.44
Gross Weight (w/ 5% Margin of Empty Weight)	**46,827.58**	21,240.99

Table 11.1: *Karfi* Mass Breakdown

The lateral position of the center of gravity is symmetric about the aircraft and does not change when in helicopter or forward flight modes. The longitudinal position of the center of gravity has a very small change of position when in helicopter or forward flight mode. The shift in position is due to the rotation of the nacelles for helicopter or forward flight modes respectively and also the reduction of fuel weight as the

mission progresses. The Karfi was designed in such a way as to minimize the shift of the center of gravity by locating the fuel tanks at the center of gravity of the aircraft and locating the nacelle pivot in between the quarter chord point and the center of gravity of the aircraft.

12 Summary and Conclusion

In response to the RFP for the 2022-2023 VFS Student Design Competition, sponsored by Sikorsky Helicopters, the University of Maryland undergraduate design team presents Karfi. The team was tasked with designing a HSVTOL cargo aircraft for use in highly contested environments and on unprepared landing surfaces. "Karfi" is the Norse word for a mid-sized cargo or troop ship. Just as the Vikings demonstrated never-before-seen naval capabilities, Karfi will revolutionize high-speed flight.

Karfi's Thrust-Compounding Tiltrotor design contains many novel technologies and improvements on current concepts. Sizing the turboshaft engines solely for hover provided substantial weight savings rather than requiring the proprotors to work efficiently in both the hover and high speed conditions. Judicious use of the fuselage-mounted turboshaft engines increases wing bending frequency and whirl flutter onset speed while also reducing the aircraft power required in forward flight. Karfi's two-speed transmission reduces the proprotor RPM in forward flight to keep the rotor tip Mach number below the transonic threshold; most of the rpm reduction takes place in the wingtip nacelle, reducing the driveshaft weight substantially. In forward flight the proprotor thrust is compounded with empennage-embedded turbofan engines which reduce the frontal area of the aircraft and intake the boundary layer of the fuselage for increased thrust efficiency. The fuselage structure was designed with lightweight isotruss longerons to handle the loads of a high-speed vehicle while minimizing the weight of the aircraft. The cabin houses a large cargo bay with a rear loading ramp for convenient loading and unloading of the payload. Karfi's wings are a reduced 17.9% t/c which provides a large drag reduction compared to other tiltrotor aircraft. The thin wing is supported by its strong and stiff graphite-epoxy torque box. The RFP emphasized the importance of controlling the downwash and outwash effects that often result from HSVTOL vehicles, and the Karfi successfully limits its disk loading to 19.5 lb/ft^2 (933.6 Pa).

References

[1] Weiner, E. e. a., "HeliX Ahead of the Curve, UMD Graduate Design Report 2013," Tech. rep., 2013.

[2] Scott, M. W., "Technology Needs for High Speed Rotorcraft," *NASA Contractor Report 177590*, 1991.

[3] Carlton, J., *Marine propellers and propulsion*, Butterworth-Heinemann, 2018.

[4] Norris, G., "Evolutionary Trail Of The Open-Fan Engine," `https://aviationweek.com/aerospace/evolutionary-trail-open-fan-engine`, 2021.

[5] Roux, E., "Modeles Moteurs," *Réacteurs double flux civils et réacteurs militairesa faible taux de dilution avec Post-Combustion. INSA-SupAéro-ONÉRA*, 2002.

[6] Han, J.-O., Shin, J.-W., Kim, J.-C., and Oh, S.-H., "Design 2-speed transmission for compact electric vehicle using dual brake system," *Applied Sciences*, Vol. 9, No. 9, 2019, pp. 1793.

[7] Harrington, A. M. e. a., "Excalibur The Cutting Edge in Tiltrotor TechnologyUMD Graduate Design Report 2011," Tech. rep., 2013.

[8] "Bell's HSVTOL Technology Development Hits New Milestone," `https://news.bellflight.com/en-US/209963-bell-s-hsvtol-technology-development-hits-new-milestone`.

[9] Munter, P., "Design and flight test of a two-speed helicopter transmission [C]," *Proceedings of the American Helicopter Society 10th Annual Forum, Wright Air Development Center*, 1954.

[10] Karem, A., "Hummingbird A160 and optimum speed rotor (OSR)," *AHS International Specialists' Meeting-Unmanned Rotorcraft: Design, Control and Testing, Proceedings*, 2005, pp. 335–356.

[11] Brown, F., Robuck, M., Kaiser, E., Ohlerking, W., Schellhase, E., Mychalowicz, E., and Paul, D., "Design and Development of a Dual Ratio Transmission for the A160T UAV Rotorcraft," *American Helicopter Society 66th Annual Forum, Phoenix, AZ*, 2010.

[12] Tishchenko, M. N., Nagaraj, V. T., and Chopra, I., "Preliminary design of transport helicopters," *Journal of the American Helicopter Society*, Vol. 48, No. 2, 2003, pp. 71–79.

[13] Johnson, W., "NDARC: NASA Design and Analysis of Rotorcraft," NASA-TP 2015–21875, Apr. 2015.

[14] Johnson, W., "NDARC-NASA design and analysis of rotorcraft validation and demonstration," *American Helicopter Society Aeromechanics Specialists"Conference*, No. ARC-E-DAA-TN1109, 2010.

[15] Nagaraj, V. T. and Chopra, I., *Preliminary Design of Rotorcraft*, Lecture Notes, ENAE 481, University of Maryland, 2023.

[16] "Advanced Deployable Compact Rotorcraft in Support of Special Operations," `https://vtol.org/files/dmfile/2006-07_sdcrfp_sikorsky.pdf`.

[17] "High Speed Vertical Takeoff and Landing (HSVTOL) Aircraft," `https://vtol.org/files/dmfile/rfp_sikorskyhvstol_40thsdc_2022-23_final.pdf`.

[18] Nagaraj, V. T., Chopra, I., and Pines, D. J., *Gamera: A Human Powered Helicopter–In Pursuit of an Aviation Milestone*, American Institute of Aeronautics and Astronautics, Inc., 2021.

[19] Leishman, G. J., *Principles of helicopter aerodynamics with CD extra*, Cambridge university press, 2006.

[20] Madison, R. K., "Pitch Change Bearing System," Bell Helicopter Textron inc., Patent US 510259, Sep. 10, 1990.

[21] Chappell, D. and Peyran, R., "Methodology for Estimating Wing Weights for Conceptual Tilt Rotor and Tilt Wing Aircraft," *Society of Allied Weight Engineers 51st Annual Conference, Hartford,*

Connecticut, 1992.

[22] Yutko, B., Titchener, N., Courtin, C., Lieu, M., Wirsing, L., Hall, D., Tylko, J., Chambers, J., Roberts, T., and Church, C., "Design and development of the D8 commercial transport concept," *31st Congress of the International Council of the Aeronautical Sciences, ICAS 2018*, International Council of the Aeronautical Sciences, 2018.

[23] Air, U. A., "TILT ROTOR RESEARCH AIRCRAFT FAMILIARIZATION DOCUMENT," .

[24] Schrenk, O., "A simple approximation method for obtaining the spanwise lift distribution," *The Aeronautical Journal*, Vol. 45, No. 370, 1941, pp. 331–336.

[25] Bartel, M. and Young, T. M., "Simplified thrust and fuel consumption models for modern two-shaft turbofan engines," *Journal of Aircraft*, Vol. 45, No. 4, 2008, pp. 1450–1456.

[26] Zhang, J., Pan, C., and Shan, Y., "Progress in helicopter infrared signature suppression," *Chinese Journal of Aeronautics*, Vol. 27, No. 2, 2014, pp. 189–199.

[27] Holder, T. C., "TYPE-CERTIFICATE DATA SHEET," *RED*, Vol. 3, 2016, pp. 102.

[28] Roskam, J., *Airplane design*, DARcorporation, 1985.

[29] Connor, R., "Twenty Years of GPS and Instrument Flight," *Smithsonian Air and Space Museum Aeronautics Department*, Vol. 24, 2014.